

PVT Relationships for Liquid and Glassy Poly(vinyl acetate)

John E. McKinney

Institute for Materials Research, National Bureau of Standards, Washington, D.C. 20234

and

Martin Goldstein

Belfer Graduate School of Science, Yeshiva University, New York, N.Y. 10033

(January 23, 1974)

PVT measurements were made on liquid and glassy poly(vinyl acetate) over ranges of -30 to 100 °C and 0 to 800 bar (gage pressure). The data were obtained by three different thermodynamic histories: (a) variable formation pressure, (b) constant formation pressure at one atmosphere, and (c) constant formation pressure at 800 bar. In all of these the glass was formed by isobaric cooling at 5 °C/h. The salient characteristics resulting from the different histories are the following. History (a) produces a glass of structure varying with formation pressure and, hence, does not necessarily give the proper thermodynamic properties of a "single physical substance." However, the liquid-glass intersection temperature, $T_g(P)$, is an important kinetic, or relaxational, property which approximates an isoviscous state. Accordingly, the values of dT_g/dP are in close agreement with those obtained from dynamic mechanical and dielectric time-temperature-pressure superposition. Constant formation histories (b) and (c) give proper thermodynamic properties of the glasses, but very little information with respect to kinetics. Increasing the pressure at which the glass is formed increases the density of the glass (at the given cooling rate) considerably in contrast to the entropy (from other work), which appears to be essentially independent of formation pressure.

A considerable part of the paper is definitional. The results are related to other *PVT*, dynamic mechanical, dielectric, and thermodynamic measurements. Interpretations are given in terms of both phenomenological and molecular models.

Key words: Density; dilatometer; entropy; glass transition; glass; liquid; polymer; poly(vinyl acetate); *PVT*; relaxation.

Contents

	Page		Page
1. Introduction	331	c. Glass formed at 800 bar	341
2. Experimental apparatus and procedure	332	4. Evaluation of data	341
2.1. <i>PVT</i> apparatus	332	4.1. Equations of state and the ordering	
2.2. Dilatometer	333	parameter Z	341
a. Design	333	4.2. Evaluation of T_g and T_g^{**} and corre-	
b. Operating equations	333	sponding properties	343
2.3. Sample	334	4.3. T_g and the isoviscous state	345
2.4. Thermodynamic histories and relaxa-		4.4. "Permanent" densification of the glass	
tional behavior	335	and T_g^* depression	345
a. Variable formation of the glass	336	4.5. Evaluation of the first Ehrenfest relation	
b. Constant formation of the glass at		and its role in time-tempera-	
atmospheric pressure	336	ture-pressure superposition	348
c. Constant formation of the glass at		4.6. Experimental uncertainties including	
800 bar	336	estimates on T_g and T_g^*	350
3. Presentation of data	337	5. Concluding remarks	352
3.1. Liquid region	337	6. References	353
3.2. Transition region (glass formation)	337		
3.3. Glasses	339		
a. Variable formation glass	339		
b. Glass formed at atmospheric pres-			
sure	340		

1. Introduction

This work is concerned with the measurement and phenomenological evaluation of the *PVT* properties

of poly(vinyl acetate) with particular attention given to the influence of thermodynamic history. Although the properties of only one polymer were evaluated here, the general behavior and concepts are considered to be, at least in a qualitative sense, applicable to amorphous polymers and glass-forming liquids in general.

It is well known that the thermodynamic history used to form a glass has an important effect on its properties. Gee [1]¹ and Ferry, in his recent treatise [2], devote considerable discussion to this point. For example, the influence of the rate of cooling on the densification of the glass and the corresponding shift of the glass transition temperature T_g on poly(vinyl acetate) have been studied over a large range of rates by Kovacs [3]. A similar effect may be obtained by forming a glass at elevated pressures as shown by Bianchi et al. [4], and later in this paper.

In this work the densification effect, among others, has been demonstrated extensively. The influence of thermodynamic history was studied by using suitable temperature-pressure-time variations which were grouped into three distinct classes. In these the glass was always formed using the same isobaric cooling rate at atmospheric and elevated pressures, always commencing at equilibrium in the liquid region, where properties are independent of history. The properties of the corresponding glasses were obtained subsequently by relatively fast temperature-pressure changes during which properties were assumed to be independent of time due to the slowness of the viscoelastic relaxations.

The parallel method of forming the glass by isothermal compressions at nearly constant rate used in references [5-8] was not employed here; however, some correlation between results from the two types of formations is included in the discussions.

The pressure range was limited to 800 bar (gauge pressure)². Although this range may appear to be small in comparison to that obtained in some other high pressure experiments, the compressibilities of polymers are relatively large, and accordingly, large changes in the transition properties are observed with pressure. On the other hand, as will be seen, a fourfold increase in the pressure range would be useful to study some of the limiting transitional phenomena predicted by some interpretations of these and other data.

In experimental observations on liquid-glass systems, one is faced with finding a suitable or appropriate definition of the glass transition temperature. A definition of $T_g(P)$ which is unique for each substance in that it is independent of the experimental mode by which it was determined is of course not possible. Different definitions of T_g are usually not equivalent. It has been proposed that with *PVT* measurements, a pressure dependent transition temperature should be defined from the intersection of the liquid and glass surfaces in *PVT* space [3, 4, 8]. Since, in this work, the glasses were formed by different histories, the intersection temperatures at each

pressure will often take on different values, and also may have markedly different pressure dependences. In order to make appropriate distinctions, it is convenient to adopt the convention proposed by Goldstein [9], which is applicable to the histories used here. With this convention $T_g(P)$ is defined as the temperature of the liquid-glass intersection, where the glass was formed by isobaric cooling repeated at different pressures at the same constant rate. The values of $T_g(P)$ may be viewed as a set of characteristic temperatures at which a mean volume relaxation time is essentially constant as pressure is varied. Although $T_g(P)$ depends upon the rate of cooling, dT_g/dP has been found to be essentially independent of rate. The other quantity from Goldstein's convention, $T_g^*(P)$, is the temperature of the liquid-glass intersection where the glass is formed by isobaric cooling at constant rate only at one pressure, with the values at other pressures in the glassy region being obtained by extrapolation of the volume isobars. It is thus equivalent to the definition mentioned earlier (3, 4, 8). Although the values of T_g and T_g^* are identical at the formation pressure, it will be seen that dT_g/dP and dT_g^*/dP differ considerably.

The meaning of these quantities in terms of the experimental data will become clearer in later discussion. At this time it is important to remember that $T_g(P)$, as defined here, measures a relaxational or kinetic property, whereas $T_g^*(P)$ measures a thermodynamic property defined from the equations of state for the liquid and glass (in pseudoequilibrium) formed by a particular history. To the extent that the glass transition is as defined in a relaxational context, T_g may be regarded as the more significant parameter.

2. Experimental Apparatus and Procedure

2.1. *PVT* Apparatus

All of the measurements, except for the reference density determinations, were obtained by pressurized volume dilatometry. The dilatometer was placed in a pressure chamber with glass windows to permit visual observations of the height of the mercury column in the dilatometer. The chamber, in turn, was placed in a liquid thermostat, also with glass windows. The height of the mercury column was read with a cathetometer at various values of the independent variables, temperature and pressure.

A low-viscosity silicone oil capable of withstanding temperatures of 250 °C was used as a thermostating liquid over the high temperature range. At lower temperatures, where the silicone oil became too viscous, and temperature gradients became evident from striations, ethyl alcohol was used. The bath temperature was controlled by a proportional controller with a thermister element. For the isobaric cooling runs the multiturn potentiometer control was varied at constant angular velocity using a variable speed gear box driven by a synchronous motor. Since the resistance-temperature relationship is essentially linear, the bath temperature was, accordingly, varied at

¹Figures in brackets indicate literature reference at end of this paper.

²The corresponding quantity in SI units is 80 megapascal (MPa).

constant rate. At temperatures below 40 °C accurate control was made possible by using a refrigerator with an adjustable back-pressure valve located between the suction side of the compressor and evaporator coil. The valve was manually set in accordance with the heat load to be removed. Final control was established by adding the appropriate amount of heat automatically with the proportional controller. The chamber temperature was read and recorded using a chromel-alumel thermocouple located within the chamber through a pressure seal. Although it would have been marginally desirable to control the chamber with a sensing element within the chamber, this is very difficult, because of the massiveness of the chamber and the difficulties encountered in using suitable sensing elements at elevated pressures. As a result a transient was introduced in the chamber temperature when a constant rate of cooling was initiated or terminated in the bath. A steady state of 0.4 °C difference between bath and chamber temperatures at a rate of cooling of 5 °C/h was reached in about 20 min. This transient response was of no consequence in these measurements because the runs were initiated well in the liquid regions and terminated in the glass. In both of these regions the effect of thermodynamic history is insignificant over the time scales which were used. By separate experiment at atmospheric pressure at the same cooling rate, the chamber temperature (at the thermocouple) and sample temperature were found to be the same within the experimental uncertainty.

The pressure chamber with glass windows is similar to that used by Martin and Mandelkern [10]. Di(ethyl hexyl) sebacate was used as the pressure transmitting fluid. The pressure was generated by a hand screw pump and measured with a 16-in bourdon tube gage. The bourdon gage is calibrated periodically against a dead weight piston gage. In the isobaric cooling runs the pressure was held constant by manual adjustment to compensate for the pressure drop resulting from the volume contractions of the constituents in the pressure chamber. In past experience the windows were found to be in danger of fracture at pressures in excess of 1 kbar. Accordingly, for a reasonable margin of safety, the maximum pressure was restricted to 800 bar.

2.2. Dilatometer

(a) Design

The dilatometer is a composite version which is described in detail in reference [11]. Only a brief description is given here for which a schematic diagram is shown in figure 1. Mercury was used as a confining fluid. The sample of polymer (O) was inserted into thimble (M), which at high temperatures prevented the molten sample from entering bore (B). The slots (N) in the thimble facilitated evacuation after assembly of the dilatometer. Sample bore (P), which is optional, reduced the thermal relaxation time of the sample. (This is true only if a strong conductor like mercury is used, as in this case, for the confining liquid.) The sample and thimble were inserted in cavity (F) which

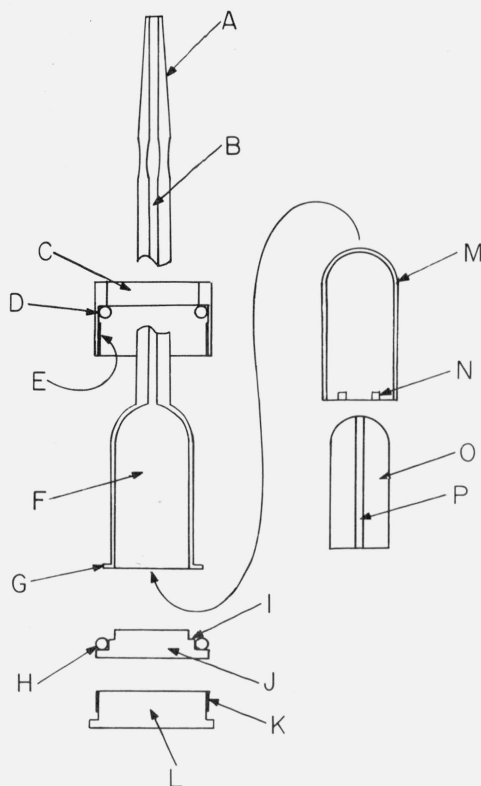


FIGURE 1. Schematic diagram of the dilatometer: (A) tapered seal, (B) capillary bore, (C-L) brass clamp, (D) rubber "O" ring, (E) female thread, (F) cavity, (G) flange, (H) rubber "O" ring, (I) mating surface, (J) stainless steel base, (K) male thread, (M) thimble, (N) slots, (O) sample, (P) sample bore.

was closed with stainless steel base (J). The base was secured by screwing a brass clamp (C-L), having very fine threads, until a seal was made completely by contact between flange (G) and surface (I). The dilatometer was then evacuated and filled with mercury. The chief advantage of a composite dilatometer with respect to polymers is that no heat sealing of the glass, from which there would be the danger of damaging the sample, is necessary. This composite dilatometer was found to be as stable over many cycles of varying temperature and pressure as the unit construction type.

(b) Operating Equations

The operating equations for the dilatometer relate the experimental observables, which are temperature, pressure, and displacement of the mercury column, to the corresponding density, or specific volume, of the sample. In the derivations of these equations it is assumed that the volumes of the dilatometer constituents are additive, and all deformations, including those of the dilatometer itself are homogeneous. The assumption of volume additivity implies that the associated compliances, $\Delta V_i/P$, are additive under hydrostatic conditions.

The total available volume V of the dilatometer up to the meniscus of the mercury column taken at some

arbitrary reference condition is

$$V_0 = (V_T)_0 + (V_S)_0 + (V_{\text{Hg}})_0 \quad (1)$$

where V_T , V_S , and V_{Hg} are the volumes of the thimble, sample and mercury at conditions T , P . The subscript 0 indicates that these quantities are taken at reference conditions T_0 , P_0 . At general conditions T , P the available volume up to the reference reading h_0 is

$$V = V_T + V_S + V_{\text{Hg}} - \pi r^2 (h - h_0) \quad (2)$$

where r is the capillary radius and h is the height of the mercury column at conditions T , P . The right-hand term is therefore the volume of mercury above the reference reading. The temperature and pressure dependences of the dilatometer glass contained in the terms $V - V_T$ and r may be expressed explicitly by rewriting eq (2) as

$$V_S = x^3 (V - V_T)_{25} - V_{\text{Hg}} + \pi x r_{25}^2 (h - h_0) \quad (3)$$

where x is an effective extension ratio approximated linearly by

$$x^3 = 1 + \alpha_D (T - 25) - \beta_D P.$$

The values $\alpha_D = 0.99 \times 10^{-5} \text{ } ^\circ\text{C}^{-1}$ [12] and $\beta_D = 2.92 \times 10^{-5} \text{ bar}^{-1}$ [13], taken as constants, are the thermal expansivity (cubic) and compressibility of borosilicate glass taken at 25 °C.

The linear dependence of the right-hand term of eq (3) on x results from the fact that the radius and the distance between any two graduations on the capillary both vary linearly with x . Accordingly, the multiplying factor is $x^2/x = x$. If the readings were read solely with a cathetometer (at ambient conditions) the right-hand term would depend upon x^2 . In our work the cathetometer was used only to interpolate between adjacent graduations.

From eq (3) the volume available for the sample and mercury at reference conditions is

$$(V_S)_0 + (V_{\text{Hg}})_0 = x_0^3 (V - V_T)_{25}.$$

This result is used to eliminate $(V - V_T)_{25}$ in eq (3). With some rearrangement and division by W_s , the sample mass, the final, desired result for the sample specific volume is obtained:

$$v_s = \frac{1}{W_s} \left\{ V_{S0} - [V_{\text{Hg}} - (V_{\text{Hg}})_0] - \left(1 - \frac{x^3}{x_0^3} \right) [(V_{\text{Hg}})_0 + (V_S)_0] + \pi x r_{25}^2 (h - h_0) \right\}. \quad (4)$$

In the above equations the contributions to the sample volume given by the terms in the braces may be identified as the reference sample volume, the change in the total volume of mercury, the change in the available volume of the dilatometer up to h_0 , and the volume of mercury above h_0 .

Since the thimble is made from the same material (borosilicate glass) as the dilatometer, V_T does not enter into equation (4).

The values for the specific volume of mercury were taken from the data of Carnazzi [14].

2.3. Sample

All measurements were made on a single sample of high molecular weight poly(vinyl acetate), grade AYAT, supplied by the Plastics Division of the Union Carbide Company.³ The intrinsic viscosity $[\eta]$ is given as 0.69 dl/g at 20 °C in cyclohexanone. The corresponding molecular weight may be estimated from the Mark-Houwink Equation [15],

$$[\eta] = KM_v^\alpha$$

where M_v is the viscosity average molecular weight. The values $K = 15.8 \times 10^{-5} \text{ dl/g}$ and $\alpha = 0.69$ are taken from reference [16] which apply to acetone solutions at 20 °C. Since acetone and cyclohexanone have the same solubility parameter, $\delta = 9.9$ [17], it is expected that the above values of K and α are applicable to cyclohexanone solutions to within the accuracy desired here. Using these values in the above equation, the value $M_v = 189,000$ was obtained for this sample. The viscosity-average lies between the number- and weight-average molecular weights, but is usually closer to the weight-average.

The above value of M_v is expected to be sufficiently high for T_g to be essentially independent of molecular weight. The validity of this assumption is indicated from the relation [18]

$$T_g = T_{g\infty} - \frac{K'}{M}$$

where M is the molecular weight of a monodisperse polymer. From references [19] and [20]⁴ experimental values of K' , ranging over a factor of two, may be approximated by 1.0×10^5 for the several polymers investigated. Although poly(vinyl acetate) was not included in the above investigations, it seems reasonable to assume that this value of K is also roughly applicable to this polymer. Using the values $K' = 1.0 \times 10^5$ and $M = 190,000$ in the above equation, the difference between T_g and $T_{g\infty}$ is only 0.5 °C, which is generally within the range of experimental uncertainty.

Since the presence of even small traces of residual solvent lowers the value of T_g considerably [21], the following procedure was used to remove the solvent.

The PVAc pellets which averaged about 5 mm in diameter were placed in a cylindrical glass tube with a tapered seal and diameter slightly larger than the thimble shown in figure 1. The tube containing the sample was evacuated to less than one torr (133 Pa)

³ Commercial material used in this experiment does not imply recommendation or endorsement by the National Bureau of Standards, nor does it imply that the material identified is necessarily the best available for the purpose.

⁴ The value of $K' = 1.2 \times 10^5$ for poly(tetramethyl-*p*-silphenylene)-siloxane is not given explicitly in this reference, but was obtained from calculations on data obtained therein.

and brought up to 120 °C using a silicone oil bath. These conditions were maintained for about three weeks, which was more than sufficient time for the sample weight to stabilize. The loss of weight over the entire process was about 1 percent, which is attributed to residual solvent. During this period the pellets flowed together and the sample assumed the shape of the container. Over several days the sample was cooled to room temperature. The tube was broken, and one end of the sample was faced on a lathe to a length slightly shorter than the thimble. A two millimeter hole was drilled through the sample, as shown in figure 1, in order to shorten the time to reach thermal equilibrium. The final dimensions of the sample shown on figure 1 are 35 × 15 mm diam with a 2 mm diam bore.

A reference value of the specific volume for the polymer was obtained using the usual hydrostatic weighing procedure [22]. A value of 0.8487 cm³/g at 40 °C was obtained after making the air buoyancy corrections [23]. 40 °C is a high enough temperature for the sample to reach viscoelastic equilibrium in a short time and low enough not to unduly complicate the hydrostatic weighing procedure.

2.4. Thermodynamic Histories and Relaxational Behavior

As stated earlier the thermodynamic history of a polymer, or glassforming liquid, has considerable influence on the experimental properties in the transition and glass regions. In this work comparisons were made between data obtained from the histories used to form the glass. All of these involved commencing a "run" at true equilibrium in the liquid region, where the properties are independent of history, and forming the glass isobarically at different pressures at a constant rate of cooling at 5 °C/hr. This rate is small enough to essentially maintain thermal equilibrium within the sample. The constant rate was terminated at some temperature well within the glassy region characterized by viscoelastic relaxation times sufficiently long in comparison to experimental times that no further changes in density with time at constant temperature were observed. Subsequent measurements in the glass were taken by an accelerated procedure.

A typical volume-temperature curve obtained by isobaric cooling at constant rate, used to form the glass, is shown schematically on figure 2a. The glass temperature, T_g , is manifested here by the rapidly changing slope as shown. In the liquid region at temperatures well above T_g , for example T_a , the time-dependent response in volume resulting from a sudden change in temperature or pressure is shown on figure 2b, where two relaxation⁵ processes may be realized. The first is a viscoelastic, or structural relaxation, which may be completed so rapidly at very high temperatures that it will not be observed by this technique. The second is a thermal relaxation, which results from a time dependent macroscopic distribution of

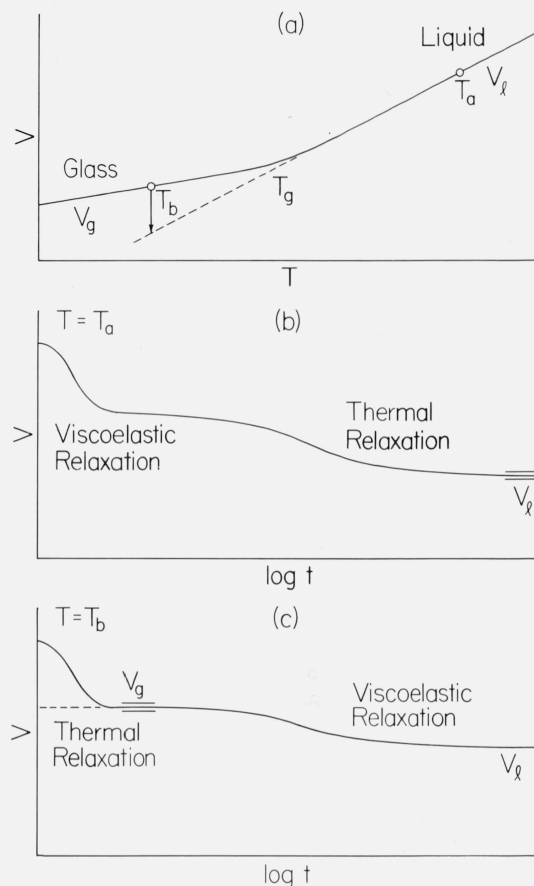


FIGURE 2. Relaxational Response in Liquid and Glass.

temperatures and corresponding densities over the sample and apparatus components equilibrating through heat transfer. The information obtained from thermal relaxations is of no interest here. In our work the thermal relaxations equilibrated in about 20 min essentially independent of temperature and pressure. At the conclusion of both relaxations the true equilibrium value, V_l , was obtained. A set of values in the liquid region was obtained by rapidly changing the temperature or pressure to the desired values and allowing true equilibrium to be attained at each point. This procedure reaching either true or apparent equilibrium at each point is referred to here as the temperature-pressure jump method.

As a result of the large increase in viscoelastic relaxation times with decreasing temperature and the constancy of the thermal relaxation times, the order of the two relaxation processes is reversed at temperatures well below T_g . Figure 2c shows the time-dependent response resulting from thermodynamic response in the glass, say at T_b , on figure 2a. The thermal relaxation is completed in about the usual 20 min followed by the viscoelastic one which may be extended over many years depending upon the temperature and pressure. Since the observed volume is essentially stationary during and well after the thermal relaxation, the value of volume obtained at the completion of the thermal relaxation appears to have reached

⁵ More strictly, "retardation" is used to express time-dependent strain at constant stress in contrast to "relaxation" for time-dependent stress at constant strain. In this work "relaxation" is used in a more general sense to cover both.

equilibrium over ordinary experimental time scales. Accordingly, this value is referred to as the pseudo-equilibrium value for the glass and is taken to be the initial value V_g for the viscoelastic relaxation as indicated by the dashed line. A set of values of V_g at different conditions are, therefore, considered as isochronal at zero time with respect to the viscoelastic relaxations. The apparent stability in V_g implies that a set of these data are representative of a thermodynamically reversible system, i.e., one for which the data are independent of the thermodynamic path by which they are obtained after the glass was formed. Note that in order to obtain a value of V_g , the relaxation processes must be distinct. When this was true, it was not practical to obtain V_l because of the large experimental times required. Accordingly, it was not practical with our equipment to obtain both V_l and V_g at the same conditions. The parallel lines at V_l and V_g indicate regions where the proper values of these quantities are obtained within the precision of the experiment. This region for V_g is finite, while the one for V_l is, of course, extended to $t \rightarrow \infty$.

No effort was made to obtain relaxational data between V_l and V_g . Volume relaxational data have been obtained over extensive ranges of temperature and pressure on polystyrene over periods up to 25 hours by Goldbach and Rehage [24]. In our work when any viscoelastic response was observed in the glass at temperatures close to T_g , the glass was reheated to the liquid condition and then reformed by the same history before subsequent data were taken.

In view of these remarks the three histories used to form the glass are described below.

a. Variable Formation of the Glass

A schematic diagram of the variable formation history (a) is given in figure 3a. The measurements were commenced at an elevated temperature sufficiently high to be in the equilibrium region at some arbitrary pressure P_i . The sample was then cooled isobarically at 5°C/hr through the apparent $T_g(P)$ to a terminal temperature well below this where the structure is "frozen in." Subsequent pseudo-equilibrium measurements in the glass were taken isobarically at P_i using the temperature jump method with regular checks on the reproducibility to insure that viscoelastic relaxations have not occurred. The same procedure was repeated at different pressures until the desired data were obtained. All pressure changes were made in the liquid state.

b. Constant Formation of the Glass at Atmospheric Pressure

History (b) (constant formation at atmospheric pressure) is illustrated schematically in figure 3b. The glass was formed in the same manner as the previous case except that isobaric cooling was at atmospheric pressure only. After the terminal temperature within the glass was reached, pseudo-equilibrium measurements were taken using the temperature-pressure jump method with regular checks to insure the absence of significant viscoelastic relaxations. All pressure changes were made in the liquid state.

c. Constant Formation of the Glass at 800 Bar

The schematic diagram for history (c) (constant formation at 800 bar) is shown in figure 3c. With this history the glass was formed in the same manner as

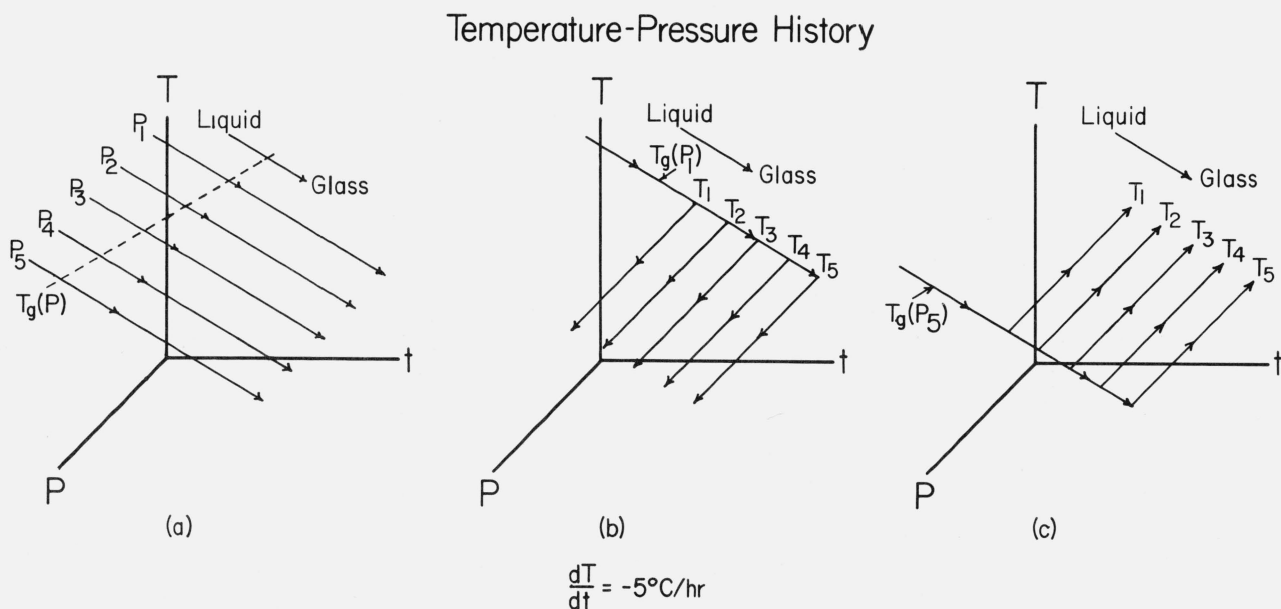


FIGURE 3. Thermodynamic histories used to form the glass: (a) variable formation, (b) glass formed at atmospheric pressure, and (c) glass formed at 800 bar.

the previous one (b) except that the isobaric cooling was at 800 bar. Pseudoequilibrium measurements within the glass were again obtained by the temperature-pressure jump method. Although the "jumps" in the glass in both histories b and c are shown schematically as isothermal, actual paths followed were not necessarily isothermal, the exact thermodynamic path in the glassy region being irrelevant over these experimental time scales.

Note that a principal distinction between the variable formation history (a) and the constant formation histories (b and c) is that with the former, all pressure changes are made in the liquid, and with the latter, all pressure changes are made in the glass.

3. Presentation of Data

3.1. Liquid Region

The liquid *PVT* data are given in table 1. All of these values are displayed by open circles on the right-hand sides of each of figures 4, 5, and 6. (These points are the least obscured from other data sets in fig. 6.)

The liquid measurements were taken by the temperature-pressure jump method. At the higher temperatures one-half hour was allowed to attain equilibrium after each jump. Since thermal relaxations equilibrated in about 20 min independent of conditions, the one half hour used here was more than sufficient. In other cases, at lower temperatures, where viscoelastic relaxations were apparent at longer times, as such as four hours were allowed to attain equilibrium. Data which did not equilibrate within this period were excluded from the set.

3.2. Transition Region (glass formation)

The data resulting from the isobaric cooling paths at 5 °C/hr, used to form the glass, are tabulated in table 2 and illustrated in figure 4 with solid circles. In all cases the measurements commenced at equilibrium in the liquid region and terminated well in the glass where viscoelastic relaxation times were large in comparison to experimental times. In the liquid region there was, of course, no distinction observed between a datum obtained by the isobaric cooling method and the temperature-pressure jump method.

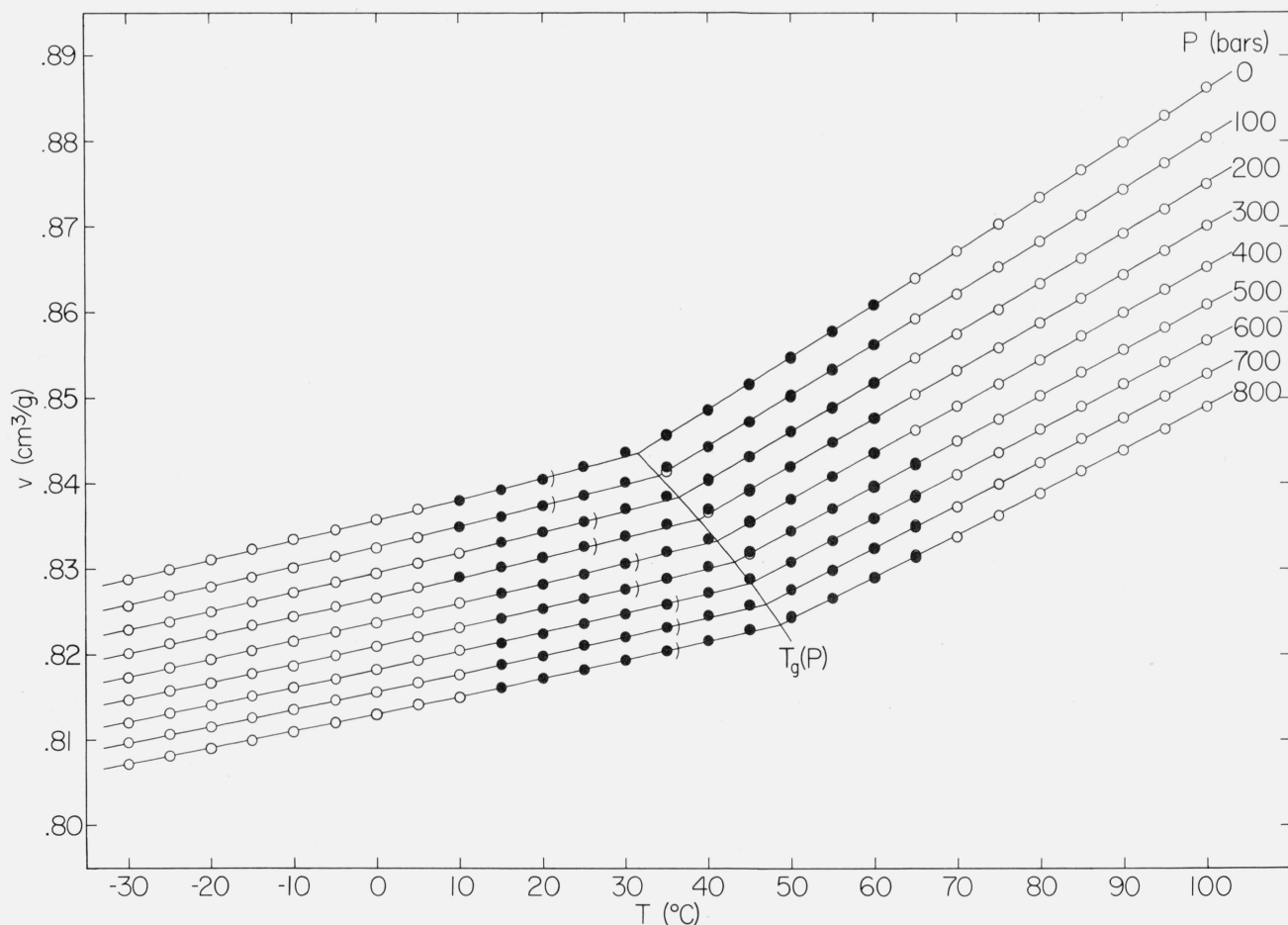


FIGURE 4. Specific volume versus temperature at different pressures using the variable formation history (a) to form the glass.

TABLE 1. *Specific volume data for the liquid region*

$T \backslash P$	0	100	200	300	400	500	600	700	800
35	0.84572	0.84148							
40	.84870	.84444	0.84041	0.83670					
45	.85174	.84733	.84321	.83921	0.83549	0.83184			
50	.85486	.85041	.84608	.84206	.83817	.83447	0.83087	0.82757	
55	.85791	.85349	.84894	.84491	.84092	.83709	.83340	.82988	0.82666
60	.86104	.85628	.85179	.84769	.84367	.83980	.83607	.83256	.82904
65	.86407	.85933	.85472	.85052	.84648	.84250	.83874	.83523	.83174
70	.86723	.86218	.85755	.85324	.84913	.84507	.84108	.83734	.83378
75	.87038	.86536	.86038	.85594	.85171	.84762	.84367	.84000	.83626
80	.87343	.86829	.86342	.85881	.85453	.85036	.84641	.84257	.83889
85	.87669	.87140	.86636	.86169	.85728	.85308	.84911	.84532	.84155
90	.87986	.87438	.86923	.86444	.86000	.85574	.85172	.84776	.84396
95	.88301	.87741	.87207	.86722	.86269	.85823	.85424	.85025	.84641
100	.88622	.88043	.87500	.87012	.86534	.86095	.85678	.85284	.84904

Units: T in $^{\circ}\text{C}$, P in bars, v in cm^3/g .

TABLE 2. *Specific volume data for the transition region*

$T \backslash P$	0	100	200	300	400	500	600	700	800
65						0.84235	0.83853	0.83500	0.83150
60	0.86094	0.85634	0.85193	0.84769	0.84362	.83973	.83602	.83248	.82912
55	.85782	.85329	.84903	.84489	.84094	.83710	.83343	.82999	.82670
50	.85468	.85023	.84615	.84208	.83819	.83446	.83094	.82772	.82461
45	.85165	.84733	.84331	.83938	.83564	.83213	.82898	.82594	.82307
40	.84861	.84443	.84061	.83710	.83360	.83039	.82732	.82467	.82176
35	.84578	.84199	.83864	.83534	.83205	.82904	.82600	.82330	.82055
30	.84374	.84023	.83706	.83392	.83069	.82776	.82482	.82216	.81948
25	.84209	.83874	.83559	.83266	.82950	.82663	.82363	.82111	.81830
20	.84061	.83747	.83436	.83145	.82831	.82542	.82250	.81995	.81728
15	.83937	.83622	.83319	.83033	.82720	.82434	.82142	.81892	.81622
10	.83812	.83503		.82915					

Units: T in $^{\circ}\text{C}$, P in bars, v in cm^3/g .

TABLE 3. *Specific volume values for the variable formation glass*

$T \backslash P$	0	100	200	300	400	500	600	700	800
-30	0.82884	0.82573	0.82292	0.82019	0.81735	0.81472	0.81206	0.80971	0.80723
-25	.83002	.82693	.82381	.82130	.81848	.81580	.81321	.81072	.80823
-20	.83110	.82797	.82503	.82236	.81944	.81672	.81412	.81166	.80910
-15	.83238	.82910	.82619	.82345	.82048	.81780	.81517	.81260	.81003
-10	.83350	.83019	.82734	.82453	.82156	.81876	.81621	.81364	.81108
-5	.83467	.83146	.82849	.82568	.82270	.81993	.81725	.81472	.81210
0	.83581	.83250	.82957	.82666	.82377	.82098	.81831	.81569	.81310
5	.83706	.83375	.83074	.82791	.82497	.82211	.81941	.81680	.81424
10	.83812	.83503	.83191	.82915	.82608	.82321	.82058	.81786	.81509
15	.83937	.83622	.83319	.83033	.82720	.82434	.82142	.81892	.81622
20	.84061	.83747	.83436	.83145	.82831	.82542	.82250	.81995	.81728
25			.83559	.83266	.82950	.82663	.82363	.82111	.81830
30					.83069	.82776	.82482	.82216	.81948
35							.82600	.82330	.82055

Units: T in $^{\circ}\text{C}$, P in bars, v in cm^3/g .

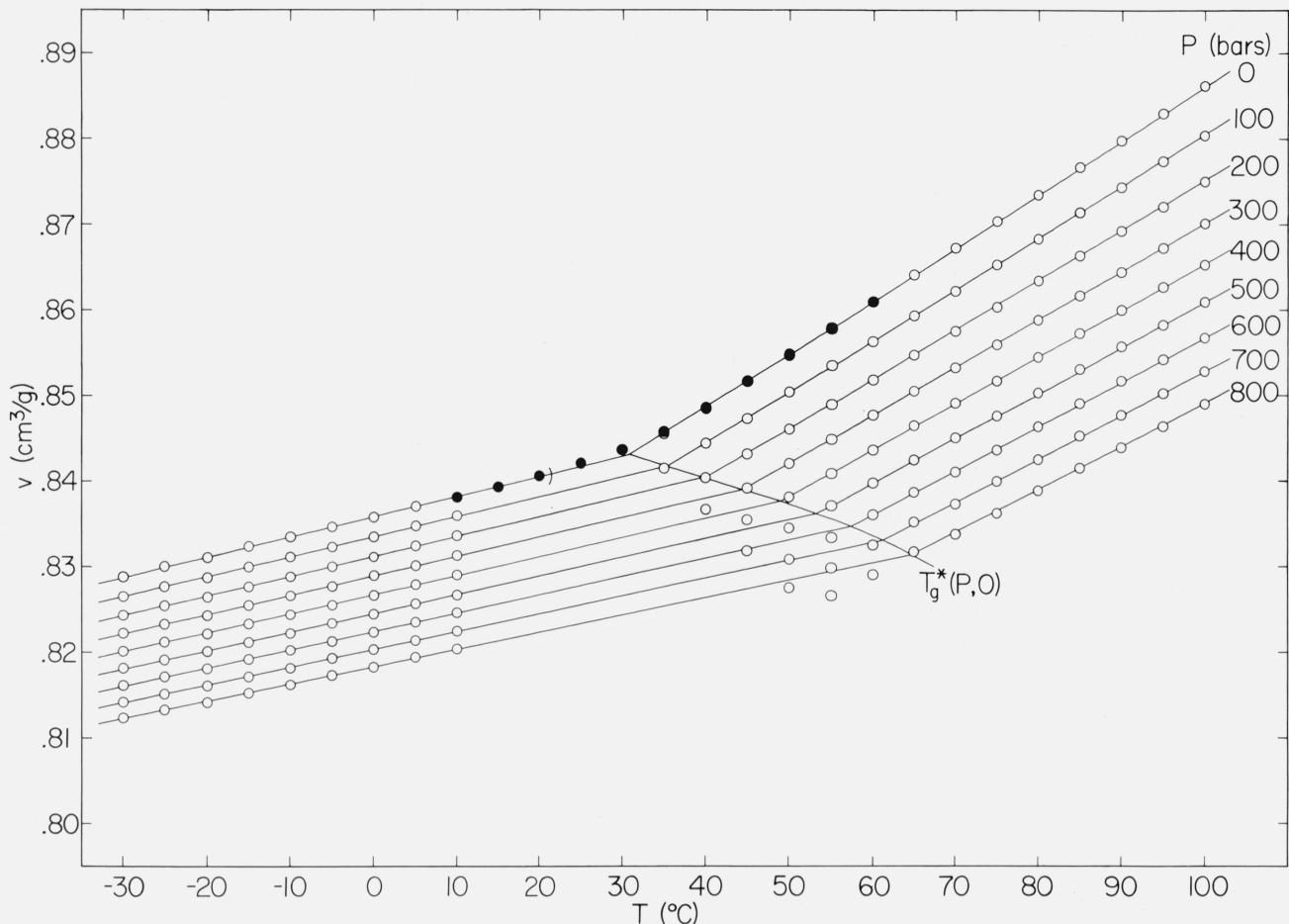


FIGURE 5. Specific volume versus temperature at different pressures using the atmospheric pressure history (b) to form the glass.

TABLE 4. Specific volume values for the one atmosphere glass

T	P	0	100	200	300	400	500	600	700	800
-30		0.82884	0.82654	0.82438	0.82225	0.82017	0.81816	0.81613	0.81419	0.81237
-25		.83002	.82768	.82547	.82334	.82121	.81914	.81715	.81516	.81327
-20		.83110	.82874	.82648	.82430	.82218	.82010	.81808	.81606	.81415
-15		.83238	.82997	.82767	.82549	.82331	.82117	.81919	.81717	.81522
-10		.83350	.83117	.82886	.82663	.82443	.82224	.82022	.81817	.81620
-5		.83467	.83233	.83003	.82774	.82557	.82340	.82131	.81933	.81729
0		.83581	.83351	.83115	.82889	.82666	.82447	.82237	.82033	.81825
5		.83706	.83478	.83241	.83012	.82794	.82569	.82355	.82140	.81941
10		.83812	.83593	.83359	.83130	.82903	.82679	.82465	.82248	.82040
15		.83937								
20		.84061								

Units: T in $^{\circ}\text{C}$, P in bars, v in cm^3/g .

3.3. Glasses

a. Variable Formation Glass

The PVT data for the glass formed by history a, using all of the formation paths included in table 2, are given in table 3. All of the measurements in the glass were taken isobarically by the temperature jump

method allowing at least one half hour to equilibrate. These data are illustrated in figure 4 by all of the points to the left of the parenthesis. Since some of the solid circles (isobaric cooling at constant rate) are representative of pseudoequilibrium, these were included in this set. The isobaric cooling data at these conditions were in agreement with those taken by the temperature jump method.

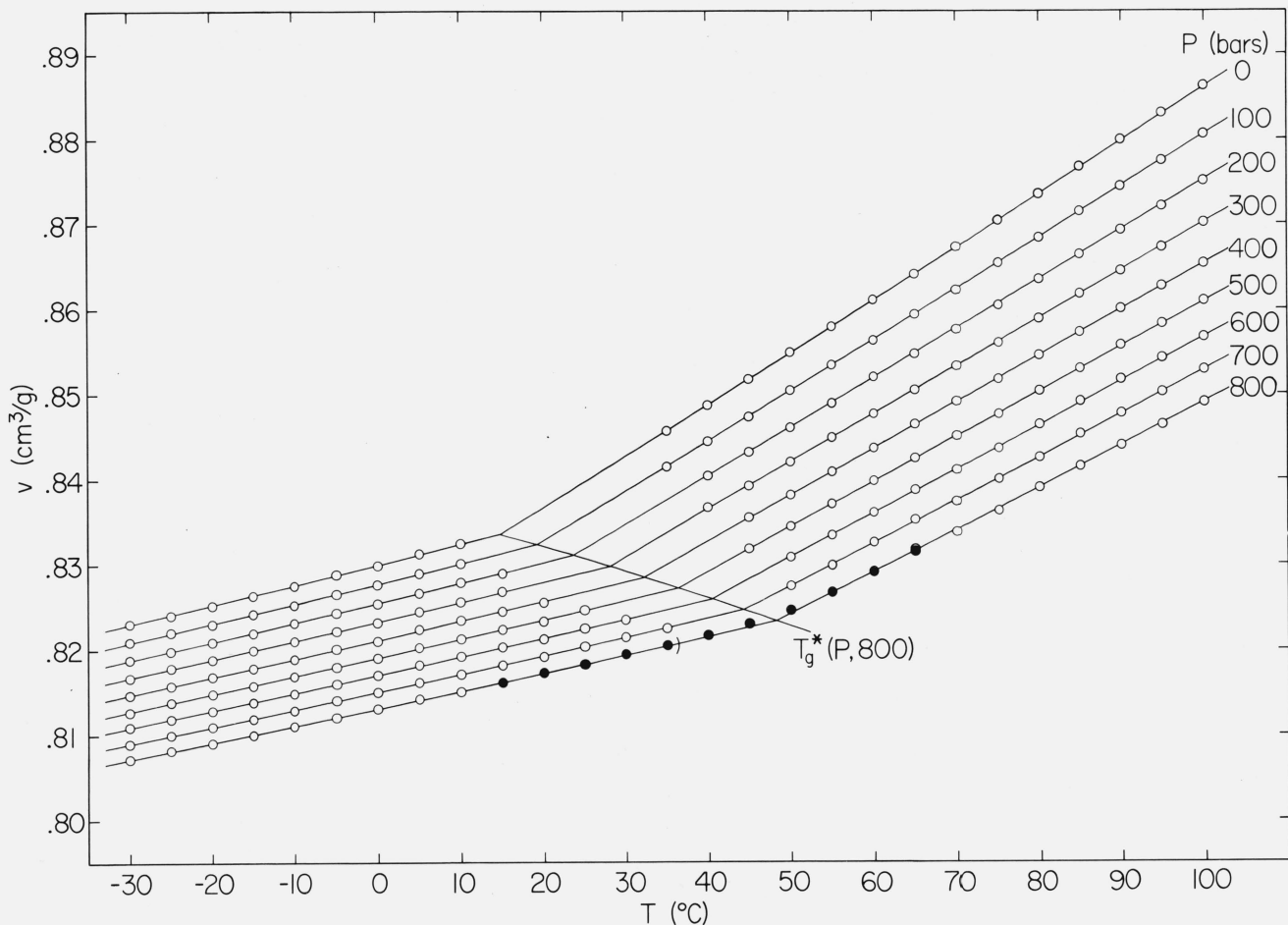


FIGURE 6. Specific volume versus temperature at different pressures using the 800 bar history (c) to form the glass.

TABLE 5. Specific volume values for the 800 bar glass

$T \backslash P$	0	100	200	300	400	500	600	700	800
-30	0.82311	0.82100	0.81886	0.81676	0.81476	0.81274	0.81087	0.80901	0.80723
-25	.82414	.82207	.81991	.81792	.81585	.81388	.81190	.81004	.80823
-20	.82526	.82308	.82097	.81891	.81688	.81484	.81291	.81101	.80910
-15	.82642	.82427	.82203	.81999	.81791	.81585	.81387	.81192	.81003
-10	.82758	.82533	.82321	.82107	.81898	.81693	.81493	.81294	.81108
-5	.82889	.82663	.82440	.82227	.82018	.81804	.81605	.81410	.81210
0	.82993	.82769	.82547	.82335	.82126	.81911	.81704	.81507	.81310
5	.83133	.82900	.82671	.82457	.82244	.82033	.81827	.81620	.81424
10	.83249	.83016	.82794	.82567	.82350	.82132	.81926	.81716	.81509
15			.82901	.82683	.82456	.82241	.82034	.81821	.81622
20					.82557	.82335	.82127	.81919	.81728
25						.82466	.82254	.82039	.81830
30							.82354	.82148	.81948
35								.82257	.82055

Units: T in $^{\circ}\text{C}$, P in bars, v in cm^3/g .

b. Glass Formed at Atmospheric Pressure

The PVT data for the glass formed by history b (isobaric cooling at atmospheric pressure) are given

in table 4. The formation data are given in column 1 of table 2. The glass data is shown in figure 5 by the open circles to the left of T_g^* and the three solid circles to the left of the parenthesis. The data shown by open

circles were obtained by the temperature-pressure jump method, and those with solid circles by constant rate of cooling at 5 °C/hr. Although in figure 3b these jumps are illustrated as isothermal at the elevated pressures, the thermodynamic path in the glass was found to have no influence on the data. In some observations at the higher temperatures where some irreversibility resulting from viscoelasticity was observed, the glass was reformed by the same history before subsequent measurements in the glass were taken.

c. Glass Formed at 800 Bar

The procedure for history c (isobaric cooling at 800 bar) is essentially the same as that for history b except the glass was formed at 800 bar. The *PVT* data for the glass are contained in table 5 with the formation data contained in the last column of table 2. The data for the glass are illustrated in figure 6 by the open and solid circles to the left of the parenthesis. The principal difference between the results from histories b and c is that the higher formation pressure produces a more densified glass with corresponding shift in $T_g^*(P)$ to lower temperatures. With history c it was possible to obtain pseudoequilibrium data closer to T_g^* . This difference may be attributed largely to experimental procedure. In approaching T_g^* from the glassy region it is desirable to take successive observations in such a way that relaxation times are always decreasing. Since the relaxation times increase with pressure at constant temperature, such a procedure to obtain values near T_g^* was impossible, or at least very difficult, with history b.

4. Evaluation of Data

4.1. Equations of State and the Ordering Parameter Z

PVT relations including thermodynamic equations of state are often used to facilitate the analysis of *PVT* data. A general expression applicable to both liquid and glass connected by a transition region would be very difficult to obtain. Not only would such an expression have to contain a large number of adjustable parameters to fit the complicated curvature, but it would have to contain the influence of thermodynamic history. A satisfactory alternative often used is to fit separate relations: one to the liquid and one to each of the glasses formed by a different history. The transition properties according to the more general definition of Kovacs [3], Bianchi [4] and Quach and Simha [8] may thus be evaluated at the intersection of the liquid and glass surfaces in *PVT* space.

The Tait equation [25, 26] which has two adjustable isothermal parameters has been used to fit data in both the liquid and glassy regions. (See for example references [8, 27].) Although the Tait equation gives a good fit with a small number of parameters, its

algebraic manipulation in finding some of the transition properties is very cumbersome. A polynomial approach was used here to facilitate the estimation of these properties, and in some cases, their uncertainties.

Using the OMNITAB Fit routine [28] a quadratic equation of the form

$$v = \sum_{i=0}^2 \sum_{j=0}^2 a_{ij} T^i P^j \quad (5)$$

was fitted to each of the data sets given in section 3 exclusive of the transition region. The values of the coefficients a_{ij} along with their standard deviations are given in table 6. The Sequential *F* test [29] was used to determine the significant coefficients. In cases where the test failed, the respective coefficients were set equal to zero. The solid lines with positive slope on figures 4, 5, and 6 give the values of the specific volumes calculated from the appropriate forms of eq (5).

As applied to these data the above equation is representative of thermal equilibrium in all cases. The liquid equation is a true equilibrium one independent of thermodynamic history. The equation for the various glasses are pseudoequilibrium representations applicable to "frozen in" structures resulting from the particular thermodynamic histories.

As a thermodynamic equation of state, eq (5) is applicable to the liquid region and constant formation glasses. This is not true for the variable formation glass (a) because it has a different structure for each formation pressure P' . Therefore, in this case, eq (5) gives the proper thermodynamic response only for isobaric changes with $P = P'$. Accordingly, the thermal expansions derived from eq (5) for the variable formation history are proper thermodynamic quantities, whereas the compressibilities are not because they do not apply to a "single physical substance".⁶ In order to make the distinction between the compressibilities, we will use Goldstein's convention [9] for which β_g is the proper thermodynamic isothermal compressibility of the glass and β_g^* is an apparent isothermal compressibility of the "glass" obtained from the variable formation history.

This argument applied to isothermal compression measurements where the measurements are commenced in the liquid and the glass is formed by increasing the pressure at constant temperature is analogous, but reversed. In this case the structure of the glass varies with the formation temperature T' . Accordingly, in this case, the derived compressibilities are proper thermodynamic quantities and the thermoexpansivities are not.

The pressure dependences of the isobaric thermal expansivities and isothermal compressibilities for the

⁶ Glasses formed by different thermodynamic histories may have different thermodynamic properties at the same temperature and pressure. They thus may be regarded as different substances even though they have identical chemical composition. Accordingly, the properties of a glass derived from data at different temperatures and pressures, but obtained from using only one history are said to pertain to a "single physical substance."

TABLE 6. Coefficients and their standard deviations

$$\text{for } a_{ij} \text{ in } v = \sum_{i=0}^2 \sum_{j=0}^2 a_{ij} T^i P^j$$

Liquid

$i \backslash j$	0	1	2
0	0.82496 ± .00030	-(0.396 ± .022) × 10 ⁻⁴	(0.124 ± .032) × 10 ⁻⁷
1	(.5820 ± .0092) × 10 ⁻³	-(.32 ± .65) × 10 ⁻⁷	-(.177 ± .091) × 10 ⁻⁹
2	(.294 ± .067) × 10 ⁻⁶	-(.146 ± .046) × 10 ⁻⁸	(.193 ± .062) × 10 ⁻¹¹

Glasses

(a) Variable Formation Glass

$i \backslash j$	0	1	2
0	0.835773 ± .000020	-(0.3147 ± .0011) × 10 ⁻⁴	(0.394 ± .013) × 10 ⁻⁸
1	(.24019 ± .00086) × 10 ⁻³	-(.460 ± .017) × 10 ⁻⁷	0
2	(.246 ± .023) × 10 ⁻⁶	0	0

(b) Glass Formed at Atmospheric Pressure

$i \backslash j$	0	1	2
0	0.835861 ± .000020	-(0.2375 ± .0013) × 10 ⁻⁴	(0.225 ± .016) × 10 ⁻⁸
1	(.2356 ± .0012) × 10 ⁻³	-(.217 ± .080) × 10 ⁻⁷	-(.25 ± .10) × 10 ⁻¹⁰
2	0	0	0

(c) Glass Formed at 800 Bar

$i \backslash j$	0	1	2
0	0.830031 ± .000019	-(0.22950 ± .00098) × 10 ⁻⁴	(0.225 ± .011) × 10 ⁻⁸
1	(.2393 ± .0010) × 10 ⁻³	-(.452 ± .018) × 10 ⁻⁷	0
2	(.207 ± .023) × 10 ⁻⁶	0	0

liquid and glasses formed by the three histories a, b, and c are given in tables 7 and 8. These expressions are evaluated from the appropriate operations on eq (5) to obtain

$$\alpha = (1/V) (\partial V / \partial T)_P \text{ and } \beta \text{ or } \beta^* = -(1/V) (\partial V / \partial P)_T$$

using the values of coefficients contained in table 6. The liquid and glasses were evaluated at 70 and 0 °C. The purpose for the inclusion of these tables, aside from reference purposes, is to illustrate the point of the argument given in the last two paragraphs. The values of α_g at any particular pressure are nearly independent of the histories used here, whereas the values of β_g^* for the variable formation history (a) are about 30 percent larger than the corresponding values for β_g from the constant formation histories (b and c). If the analogous procedure were conducted with isothermal compression, the corresponding variation would be in the thermal expansivities.

It has been proposed that the thermodynamic properties of liquids near T_g may be specified by an ordering parameter set $\{Z\}$, the values being functions of T and P at equilibrium, but becoming constant in the glass at the values they have at T_g . Experimental data may be used to answer two questions about such a set of

ordering parameters: first, is one sufficient, or is more than one necessary, and second, when glasses are formed at constant cooling rate (and hence at constant relaxation time) under various pressures, are the values of the Z_i 's frozen in independent of, or vary with, the formation pressure. The first is answered by testing the inequality $\Delta\beta/\Delta\alpha \geq TV\Delta\alpha/\Delta C_p$, where C_p is the heat capacity at constant pressure. If they are equal, one is sufficient [30]. In the absence of C_p data on this sample of polymer, the question cannot be answered; the evidence on a number of glass-formers available in the literature indicates that $\Delta\beta/\Delta\alpha$ is about twice $TV\Delta\alpha/\Delta C_p$, and hence a single ordering parameter is not sufficient. Incidentally the sense of the inequality

$$\Delta\beta/\Delta\alpha \geq TV\Delta\alpha/\Delta C_p$$

is based on considerations of thermodynamic stability, and must always be satisfied if the hypotheses used in obtaining the configurational properties (those prefixed by Δ) are justified. (See ref [9] for a detailed discussion.)

The fact that configurational volume is a function of P' for constant cooling rate (or in other words, two different samples of glass prepared by cooling the liquid under two different pressures at the same constant

TABLE 7. Thermal expansivities typical of the liquid and glasses a, b, and c

P bar	Liquid, 70 °C	$\alpha \times 10^4$ (°C ⁻¹)		
		Glass, 0 °C		
		a	b	c
0	7.186	2.874	2.819	2.884
100	6.963	2.829	2.798	2.837
200	6.758	2.784	2.771	2.790
300	6.571	2.739	2.737	2.742
400	6.403	2.692	2.697	2.694
500	6.253	2.645	2.650	2.646
600	6.123	2.598	2.598	2.598
700	6.013	2.550	2.538	2.548
800	5.922	2.501	2.472	2.499

TABLE 8. Compressibilities typical of the liquid and glasses a, b, and c

P bar	Liquid, 70 °C	$\beta \times 10^5$ (bar ⁻¹)		
		Glass, 0 °C		
		a	b	c
0	5.653	3.765	2.841	2.765
100	5.463	3.685	2.795	2.718
200	5.270	3.603	2.749	2.671
300	5.074	3.521	2.702	2.623
400	4.875	3.437	2.655	2.575
500	4.673	3.353	2.607	2.527
600	4.467	3.268	2.559	2.478
700	4.259	3.181	2.510	2.429
800	4.048	3.094	2.462	2.380

cooling rate, and then compared at the same T and P below T_g , have different volumes), implies that configurational volume does not determine relaxation time, and hence does not determine T_g . This is equivalent to saying that whatever ordering parameter is associated with free volume does not take a constant value independent of formation pressure (for fixed cooling rates).

In view of these remarks specification of any property of a glass requires knowledge both of the present observables (T and P) and the thermodynamic history by which the glass was formed. For example, when isobaric cooling at constant rate $k = -dT/dt$ is used to form the glass, any property may be expressed in terms of the arguments T , P , P' , and k , where T and P are the present values and P' and k specify the history. A generalized equation of state for a glass formed in this manner would be $v = v(T, P, P', k)$. For isothermal compression at constant rate the corresponding arguments would be T , P , P' , and $c = dP/dt$, where T' is the formation temperature.

4.2. Evaluation of T_g and T_g^* With Corresponding Properties

As stated in the Introduction T_g and T_g^* are defined as the temperature at the intersection of the liquid and appropriate glass surfaces in PVT space, where T_g

is obtained from the variable formation glass (a), and T_g^* is obtained from either of the constant formation glasses (b or c). T_g^* will of course take on different values for the two glasses. In general for these histories, the above definitions imply that at the intersection temperature $T(\Delta V = 0)$, where $\Delta V = V_l - V_g$,

$$T(\Delta V = 0) = T_g^*(P, P'),$$

and

$$T(\Delta V = 0) = T_g(P), \text{ when } P = P'.$$

Accordingly, $T_g = T_g^*$ only when $P = P'$, as is always true with the variable formation history (a). Since T_g is a function of only one independent variable (since the cooling rate was the same in all cases) T_g appears to be unique while T_g^* is not.

The temperature of intersection for each history may be obtained by equating the right-hand sides of the two forms of eq (5) with appropriate coefficients for liquid and glass taken from table 6. The solution for T_g or T_g^* is quadratic in P , but only one branch is appropriate in the physical sense over the experimental pressure range. These transitions are illustrated by the solid lines with negative slopes in figures 4, 5, and 6. Other pressure dependent properties may thus be obtained at the intersection from the appropriate manipulation of these equations with $T = T_g$ (or T_g^*) without resorting to numerical or graphical methods, as is often done using the Tait Equation.

Quach and Simha [8] have used an interesting approach to define and determine glass transition temperatures from their data on polystyrene. They used two methods to evaluate these characteristic temperatures from the same set of data, which were obtained using the following procedure. Commencing in the liquid region, the sample was cooled isobarically at atmospheric pressure at a rate of 10 °C/h to some terminal temperature T_i . At T_i the procedure was changed to isothermal compression at approximately 400 bar/h. This procedure was repeated at successively lower values of T_i . Accordingly, for values of $T_i < T_g(0)$, the glass was formed by isothermal compression and $T_g(P)$ was defined from the pressure at which the derivative of the compressibility went through a maximum along isotherm T_i . They call the glass obtained from the data at pressures above that for the compressibility slope maximum, the "high pressure glass." In the other case ($T_i < T_g(P)$), where the glass is formed at atmospheric pressure, $T_g(P)$ (their definition) was defined from the intersection of liquid and glass surfaces. They call this glass the "low pressure glass."

In making the comparison between the terminology used in their and our work, Quach and Simha's "high pressure glass" is nearly analogous to our "variable formation glass." It turns out that T_g determined from the maximum in compressibility slope nearly corresponds to that from the liquid glass surface intersection obtained from the same data. Accordingly, their "high pressure glass" is formed by isothermal compression

sion at different temperatures whereas our "variable formation glass" is obtained by isobaric cooling at different pressures. Both of these histories produce glasses with varying structure. Their "low pressure glass" corresponds directly to our "constant formation at atmospheric pressure," with their "low pressure" T_g corresponding to our T_g^* .

The values of T_g and T_g^* and other properties at these conditions as functions of pressure for these histories are given in table 9. These properties include the specific volume v , liquid and glass thermal expansivities α_l and α_g and compressibilities β_l and β_g or β_g^* . In keeping with the convention used by Goldstein [9] the * used in connection with the compressibility indicates that it is not a proper thermodynamic property. In this work β_g^* designates the apparent compressibility for the "variable formation glass (a)" which is not a single physical substance. As stated earlier a corresponding distinction is not neces-

sary for the thermal expansivity when the glass is formed by isobaric cooling at constant rate. Also included in table 9 are $\Delta\alpha = \alpha_l - \alpha_g$, $\Delta\beta$ (or $\Delta\beta^*$) = $\beta_l - \beta_g$ (or β_g^*), and dT_g/dP (or $dT_g^*/dP = \Delta\beta/\Delta\alpha$ [9]).

Since a constant rate of cooling was used, T_g or T_g^* may be specified uniquely as functions of the present pressure P and formation pressure P' . The transition map shown in figure 7 gives T_g and T_g^* as a function of P with parameter P' . As pointed out in section 4.2 the variable formation history a, is the only one for which it is always true that $P = P'$. The values of dT_g/dP and dT_g^*/dP differ by nearly a factor of two. The fact that these curves do not intersect at precisely 0 and 800 bar is an artifact resulting from the statistical treatment of the data. The three curves were evaluated from three different sets of data for which glasses a and b have common specific volume values at atmospheric pressure, and a and c, at 800 bar. The corresponding intersections on figure 7 occur at these

TABLE 9. Transition parameters

(a) Variable Formation Glass										
P	T_g	v	$\alpha_l \times 10^4$	$\alpha_g \times 10^4$	$\Delta\alpha \times 10^4$	$\beta_l \times 10^5$	$\beta_g^* \times 10^5$	$\Delta\beta^* \times 10^5$	dT_g/dP	$T_g\Delta\alpha$
bar	°C	cm ³ /g	°C ⁻¹	°C ⁻¹	°C ⁻¹	bar ⁻¹	bar ⁻¹	bar ⁻¹	°C/bar	
0	31.50	.84358	7.118	3.031	4.088	4.990	3.902	1.088	0.0266	0.1245
100	34.08	.84098	6.997	3.000	3.996	4.838	3.834	1.003	.0251	.1228
200	36.53	.83840	6.850	2.969	3.881	4.690	3.766	.924	.0238	.1202
300	38.85	.83585	6.685	2.937	3.748	4.543	3.696	.848	.0226	.1169
400	41.05	.83334	6.509	2.904	3.506	4.397	3.624	.773	.0214	.1133
500	43.13	.83085	6.328	2.869	3.459	4.249	3.552	.697	.0202	.1094
600	45.08	.82839	6.148	2.834	3.314	4.098	3.478	.620	.0187	.1055
700	46.86	.82596	5.973	2.797	3.176	3.942	3.403	.539	.0170	.1016
800	48.46	.82355	5.807	2.759	3.048	3.780	3.326	.454	.0149	.0980

(b) One Atmosphere Glass										
P	T_g^*	v	$\alpha_l \times 10^4$	$\alpha_g \times 10^4$	$\Delta\alpha \times 10^4$	$\beta_l \times 10^5$	$\beta_g \times 10^5$	$\Delta\beta \times 10^5$	dT_g^*/dP^a	$T_g^*\Delta\alpha$
bar	°C	cm ³ /g	°C ⁻¹	°C ⁻¹	°C ⁻¹	bar ⁻¹	bar ⁻¹	bar ⁻¹	°C/bar	
0	30.68	.84309	7.117	2.795	4.322	4.981	2.896	2.085	0.0482	0.1313
100	35.42	.84177	6.996	2.771	4.225	4.856	2.880	1.976	.0468	.1304
200	40.05	.84042	6.840	2.740	4.100	4.743	2.869	1.874	.0457	.1284
300	44.57	.83905	6.664	2.704	3.960	4.637	2.864	1.773	.0448	.1258
400	49.00	.83765	6.480	2.662	3.818	4.532	2.864	1.668	.0437	.1230
500	53.29	.83620	6.300	2.614	3.686	4.420	2.868	1.552	.0421	.1203
600	57.39	.83468	6.136	2.559	3.576	4.298	2.877	1.421	.0397	.1182
700	61.20	.83308	5.998	2.499	3.499	4.158	2.889	1.270	.0363	.1170
800	64.61	.83137	5.894	2.433	3.461	3.999	2.903	1.096	.0317	.1169

(c) 800 Bar Glass										
P	T_g^*	v	$\alpha_l \times 10^4$	$\alpha_g \times 10^4$	$\Delta\alpha \times 10^4$	$\beta_l \times 10^5$	$\beta_g \times 10^5$	$\Delta\beta \times 10^5$	dT_g^*/dP^a	$T_g^*\Delta\alpha$
bar	°C	cm ³ /g	°C ⁻¹	°C ⁻¹	°C ⁻¹	bar ⁻¹	bar ⁻¹	bar ⁻¹	°C/bar	
0	14.75	.83361	7.085	2.944	4.141	4.849	2.833	2.016	.0487	.1192
100	19.44	.83240	7.010	2.918	4.092	4.668	2.809	1.860	.0454	.1197
200	23.87	.83115	6.885	2.890	3.996	4.511	2.783	1.728	.0433	.1187
300	28.12	.82986	6.726	2.861	3.865	4.371	2.756	1.615	.0418	.1164
400	32.25	.82856	6.542	2.832	3.711	4.244	2.728	1.516	.0409	.1133
500	36.30	.82726	6.348	2.802	3.546	4.126	2.700	1.425	.0402	.1097
600	40.29	.82596	6.153	2.771	3.382	4.010	2.672	1.338	.0396	.1060
700	44.21	.82466	5.968	2.741	3.228	3.894	2.643	1.251	.0388	.1024
800	48.02	.82335	5.804	2.709	3.095	3.773	2.614	1.159	.0374	.0994

$$^a \frac{dT_g^*}{dP} = \frac{\Delta\beta}{\Delta\alpha}$$

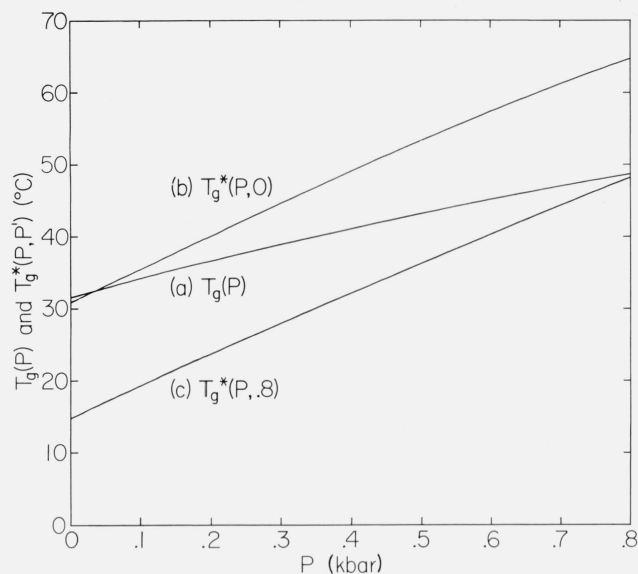


FIGURE 7. Transition map showing T_g and T_g^* versus pressure for histories (a) variable formation ($P' = P$), (b) glass formed at atmospheric pressure ($P' = 0$), and (c) glass formed at 800 bar ($P' = 800$).

values, within the 95 percent confidence limits on T_g and T_g^* (see sec. 4.6).

From a comparison of the specific volumes at T_g or T_g^* in table 9, it is seen that the constant formation histories produce a more nearly constant volume "transition" than the variable formation one. The fact is clearly evident through comparison of figures 5 and 6 with 4.

Simha and Boyer [31] have proposed a free volume model which rationalizes the observation that the quantity $T_g \Delta \alpha$ is nearly constant for different polymers. Accordingly, it appears to be appropriate to consider the constancy of $T_g \Delta \alpha$ and, possibly, $T_g^* \Delta \alpha$ over pressure for any given polymer. The values given in table 9 tend to decrease with pressure. The variation for $T_g^* \Delta \alpha$ is 11 percent (history b) compared with 21 percent for $T_g \Delta \alpha$ (history a). Similar behavior with increasing pressure was observed for polystyrene [32].

The Simha-Boyer Relation can be tested more sensitively also by examining its prediction of dT_g/dP . This has been done by Goldstein [9] using the data of this paper: the result is an over-estimate of dT_g/dP by a factor of nearly 3.

4.3. T_g and the Isoviscous State

It has been asserted that the dilatometric T_g as observed in this study corresponds, for any given liquid, to that temperature at which a characteristic value of viscosity is attained. According to Turnbull [33], a common value for the steady flow shear viscosity for simple liquids where it has been measured at T_g , is 10^{15} P. At elevated pressures the value of T_g will increase as required to maintain the isoviscous state.

With our variable formation history (a) from which

we define $T_g(P)$, the intersection of the liquid and glass PVT surfaces will occur at a temperature at which a mean volume relaxation time corresponds to the effective experimental time. This will of course depend upon the rate of isobaric cooling. Since all of the volume isobars were obtained at the same rate of cooling, T_g may be viewed upon as the temperature for constant average volume relaxation time. Accordingly, since there is very little distinction between the values of average shear and volume relaxation times at the same conditions [45], and since the relative temperature and pressure dependences of the compressibilities are small in comparison to those for shear viscosity $T_g(P)$ (from the variable formation history) should be a reasonable approximation to an isoviscous state.

Although the above assumption is plausible, it is not to be understood as an exact relationship. On the other hand, there is an independent experimental confirmation [2, 6, 34] in view of the fact that our values of dT_g/dP are in close agreement with those obtained from the shift in characteristic temperatures with pressure at constant frequency obtained through time-temperature-pressure superposition of both dielectric and dynamic mechanical data. $(\partial T/\partial P)_\omega$ has been shown to approximate the isorelaxation time or isoviscous state from both phenomenological and molecular models.

4.4. "Permanent" Densification of the Glass and T_g^* Depression

As seen from comparing the glass data of the two constant formation histories b and c, a "permanent" densification of the glass results from increasing the formation pressure. Although these glasses are not in true equilibrium, they are taken to be in pseudo-equilibrium, or as having a fixed (nonrelaxing) structure, over an observable time scale. At very long times, however, significant relaxations may occur at temperatures in the proximity of T_g . Densification has been observed on poly(methyl methacrylate) by Kimmel and Uhlmann [35] at pressures up to 50 kbar. However, at no time was the formation pressure applied entirely in the liquid region. In their work pressures were so high that permanent densification could be obtained by applying pressure in the glass. In our work no irreversible response was observed in the glass at temperatures well below T_g .

The densification effect is illustrated in figure 8 where the 0 and 800 bar curves are taken from each of figures 4 and 5 (constant formation histories b and c). The effect of increasing the formation pressure P' is to produce a permanent decrease in the specific volume of the glass with a corresponding decrease in $T_g^*(P, P')$ for a given value of P .

In this application for constant rate of cooling the densification rate (with respect to formation pressure), may be defined as

$$\beta'(T, P, P') = -\frac{1}{V} \left(\frac{\partial V}{\partial P'} \right)_{T,P}$$

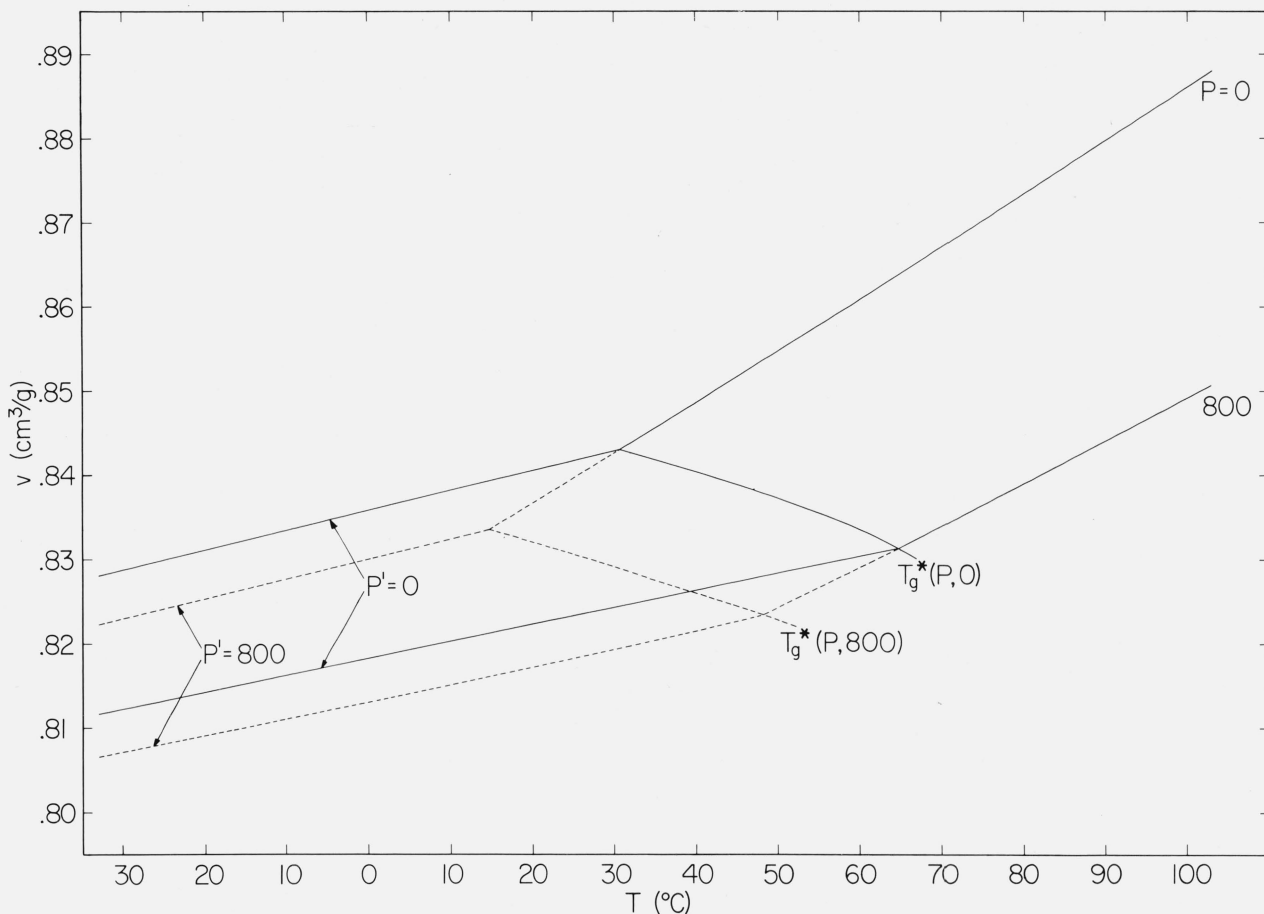


FIGURE 8. Illustration of densification and T_g^* depression from elevated formation pressures. Specific volume versus temperature at atmospheric pressure and 800 bar for constant formation histories (b) $P' = 0$ and (c) $P' = 800$ bar.

which is analogous in form to the isothermal compressibility

$$\beta(T, P, P') = -\frac{1}{V} \left(\frac{\partial V}{\partial P} \right)_{T, P'}$$

Since we have a complete description of the glass at only two values of P' (0 and 800 bar), the average of β' over P' is

$$\beta' = \frac{2[v(T, P, 0) - v(T, P, 800)]}{800[v(T, P, 0) + v(T, P, 800)]}$$

Using the values $v(0, 0, 0) = 0.83586$ and $v(0, 0, 800) = 0.83003$ cm³/g from eq (5) with appropriate coefficients from table 6 gives $\beta' = 0.88 \times 10^{-5}$ bar⁻¹. This value may be compared to the corresponding isothermal compressibility $\beta = 2.81 \times 10^{-5}$ which is the average for histories b and c at $P = 0$.

With the pressure induced densification there is a corresponding pressure induced T_g^* depression, $(\partial T_g^*(P, P')/\partial P')_P$ for which the average value over P' at $P = 0$ is $[T_g^*(0, 800) - T_g^*(0, 0)]/800$. Taking the values of T_g^* at $P = 0$ for histories b and c gives an

average value of

$$\left(\frac{\partial T_g^*(0, P')}{\partial P'} \right)_P = \frac{14.75 - 30.68}{800} = -0.020 \text{ } ^\circ\text{C}/\text{bar}$$

Note that $T_g^*(P, P')$ is increased by increasing the present pressure, but decreased by increasing the formation pressure.

As evident from figure 8 increasing the formation pressure P' produces a permanent densification and corresponding depression of the intersection temperature in a manner similar to that which would be obtained by appropriately increasing the rate of cooling k . These effects are compared schematically in figure 9, which illustrates volume-temperature curves at atmospheric pressure for the two cases: (a) that obtained from isobaric cooling at 5 °C/h at the two formation pressures, atmospheric and 800 bars, and (b) that obtained from isobaric cooling at atmospheric pressure at the two cooling rates, 5 °C/h and k_1 necessary to obtain the same value for the intersection temperature as with the 800 bar formation pressure in (a), i.e., $T_g(0, k_1) = T_g^*(0, 800, 5)$. Note that, in accordance with our convention including different constant

cooling rates, the functions T_g and T_g^* are expressed here in terms of their arguments as $T_g(P, k)$ and $T_g^*(P, P', k)$. For simplicity the volume-temperature curves on the two figures are taken to be identical; however, it is recognized that there may be some difference between the slopes of these curves for the glass formed at 800 bar (glass B) and the one formed at rate k_1 (glass C). (There is no distinction between glass A in (a) and glass A in (b).) In figure 9b the dashed line for glass C indicates behavior which could not be evaluated from these data.

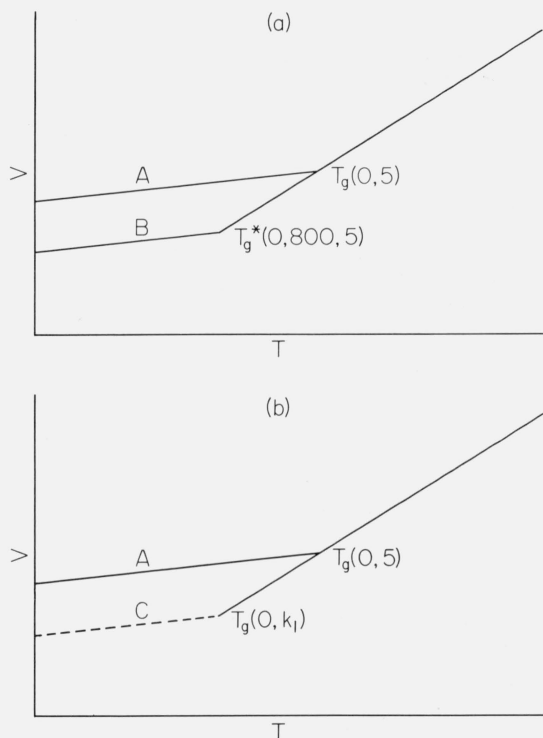


FIGURE 9. Schematic volume-temperature diagram illustrating identical volumes of glasses at $T_g(P, k)$ and $T_g^*(P, P', k)$ obtained from (a) isobaric cooling at 5 °C/h at formation pressures, 0 (Glass A) and 800 bar (Glass B), and (b) from isobaric cooling at atmospheric pressure at rates 5 °C/h (Glass A) and k_1 (Glass C) necessary for $T_g^*(0, 0, 5) = T_g(0, k_1)$.

The dashed line indicates behavior which could not be evaluated from these data.

We wish to estimate the value of k_1 necessary to make $T_g(0, k_1) = T_g^*(0, 800, 5)$ for glasses B and C, respectively. Although the validity of the WLF Equation [36]

$$\log a_T = - \frac{T - T_g}{2.303 f_g (f_g / \alpha_f + T - T_g)} \quad (6)$$

is questionable at temperatures below T_g , it may be used to obtain a crude estimate of k_1 . In eq (6) T_g is the nominal pseudoequilibrium value at atmospheric pressure which may be taken to be equal to our $T_g(0, 5)$, a_T is the ratio of relaxation times at an arbitrary temperature T to those at T_g , f_g is the free volume

fraction f at T_g , and α_f is the temperature coefficient of f . Taking $f_g = 0.028$ and $\alpha_f = 4.4 \times 10^{-4} \text{ } ^\circ\text{C}^{-1}$ from reference [37] and $T - T_g = -16 \text{ } ^\circ\text{C}$, which is the value obtained from these data by taking $T_g(0, k_1) - T_g(0, 5) = T_g^*(0, 800, 5) - T_g^*(0, 0, 5)$, gives the value of $\log a_T = 5.2$.

Assuming that the ratio of cooling rates is equal to $1/a_T$ gives a rate of $3 \times 10^{-5} \text{ } ^\circ\text{C/h}$ compared to our 5 °C/h rate. According to this model a formation pressure of 800 bar over a period of 10 h (60 to 10 °C at 5 °C/h) produces the same effect on the glass as a constant rate of cooling over 200 years at atmospheric pressure.

Although equal volumes in the glass at the same conditions can be obtained from vastly different histories, as indicated from the example above, this fact does not imply that the thermodynamic states, and hence all properties at the same volumes at the same conditions will be identical for different histories. From the Lorentz-Lorenz Equation, it is expected that increasing the density will result in a corresponding increase in the refractive index. Accordingly, it appears possible to produce glasses with higher refractive indices by increasing the formation pressure in lieu of commensurately decreasing the rate of cooling. On the other hand relaxation times for glasses of a given configurational volume obtained by slow rates of cooling would be expected to be much longer than those formed by increasing the formation pressure but keeping cooling rate constant. Since the Second Ehrenfest Relation,

$$\frac{dT_g}{dP} = \frac{TV\Delta\alpha}{\Delta C_p}, \quad (7)$$

appears to hold for most glasses examined, its obedience implies a single entropy surface for glasses obtained from different formation pressures [9]. Obedience to eq (7) does not imply, however, that there will be a single entropy surface for glasses formed at different rates of cooling. The fact that longer relaxation times are produced by cooling at a slower rate than commensurately increasing P' is related to the apparent dominance of entropy over volume in determining relaxation times. A liquid cooled under a high pressure has a lower configurational volume than one cooled at lower pressures, even though the volume relaxation time is the same for both at their respective T_g 's. To prepare a liquid by cooling at low pressure with the same volume as that achieved by high pressure cooling, one must cool very slowly, meaning that the T_g corresponds to a much longer relaxation time than the high pressure experiment. Accordingly, it appears that a more stable glass may be produced by decreasing the rate of cooling in lieu of commensurately increasing the formation pressure to obtain the same volume.

Related to the above argument is the possibility of approaching the hypothetical ground state by increasing the formation pressure. According to a theory of Gibbs and DiMarzio [38] there exists a ground state reached at temperature $T_2 > 0$ at which the configura-

tional entropy vanishes. The theory predicts that there will be a corresponding equilibrium second order transition at T_2 which, in principle, could be reached by an infinitely slow rate of cooling. From observation of figures 9a and 9b, for which the volume-temperature response is identical, one might expect to approach T_2 , and hence the ground state, by sufficiently increasing the formation pressure in lieu of decreasing the rates of cooling to values which would be impractical to attain experimentally. This possibility appears to be precluded by the apparent existence of a single entropy surface as mentioned in the last paragraph. Thus increasing the formation pressure would not enable us to come closer to the ground state, unless the relation (7) does not hold at higher pressures, or in other words, unless constant entropy does not imply constant relaxation time.

4.5. Evaluation of the First Ehrenfest Relation and Its Role in Time-Temperature-Pressure Superposition

The PVT data obtained here can be used to test the validity of the First Ehrenfest Relation

$$\frac{dT_2}{dP} = \frac{\Delta\beta}{\Delta\alpha} \quad (8)$$

where T_2 , here, is a second order transition temperature at which the free energy surfaces of two distinct thermodynamic phases are tangent along the transition line in PVT space. $\Delta\beta$ and $\Delta\alpha$ are the differences between the compressibilities and thermal expansions for the two states. The problem here is to determine the corresponding properties applicable to the glass transition and to test if eq (8) is true or not.

The evaluation of the properties that appear in eq (8) may be better realized through consideration of figure 10, which gives a schematic representation of all the PVT surfaces obtained comprising the liquid, variable formation (a), glass formed at atmospheric pressure (b), and glass formed at 800 bar (c). For simplicity all surfaces are represented by planes. The intersection designated by T_2 indicates the possibility of the existence of an equilibrium, second order transition as predicted from the theory of Gibbs and DiMarzio mentioned earlier. As indicated by figure 10, the surfaces are continuous through liquid-glass intersections as shown. The extension of the liquid surface to lower temperatures (or higher pressures) may be realized by conducting the experiments at sufficiently long time scales, as is illustrated in figure 5. In turn, extensions of the glass surfaces, may be realized through sufficiently rapid increases in temperature (or decreases in pressure) commencing in the glassy state. The glass surface extensions are very unstable, however, because of the very short viscoelastic relaxation times at these conditions, nevertheless they can be experimentally realized through, for example, ultrasonic techniques.

It has been shown by Passaglia and Martin [39], see also Goldstein [9], that if the quantities $\Delta\beta/\Delta\alpha$ or dT_g/dP are obtained by defining their values from 2 sur-

faces intersecting in 3 dimensional space, the equation will be true tautologically. To test it in a nontrivial sense is equivalent to asking if the surfaces in PVT space corresponding to glasses formed under different pressures coincide to form a single surface or not. If they had coincided the following relationships would apply

$$\Delta\beta = \Delta\beta^*$$

$$dT_g/dP = dT_g^*/dP$$

and

$$dT_g/dP = \Delta\beta/\Delta\alpha = \Delta\beta^*/\Delta\alpha.$$

Since however, our results show that the glass surfaces in PVT space do not coincide, it follows that

$$\frac{dT_g}{dP} \neq \frac{\Delta\beta}{\Delta\alpha}, \quad (9)$$

although

$$\frac{dT_g^*}{dP} = \frac{\Delta\beta}{\Delta\alpha} \quad \text{and} \quad \frac{dT_g}{dP} = \frac{\Delta\beta^*}{\Delta\alpha}. \quad (10)$$

It is possible to evaluate both terms of ineq (9) at the two points A and B (fig. 10) directly from these data. These are the triple intersection points for the (liquid-glass a-glass b) and (liquid-glass a-glass c) surfaces. (The points A and B correspond to the intersections shown on fig. 7 at 0 and 800 bar.) At point A, dT_g/dP is evaluated from the liquid-glass a intersection line, whereas $\Delta\beta/\Delta\alpha$ is evaluated from the liquid-glass b intersection line. Taking the value at $P=0$ from table 9a, we find $dT_g/dP=0.027$ °C/bar; and from the value of dT_g^*/dP at $P=0$ from table 9b and applying eq (10), we find $\Delta\beta/\Delta\alpha=0.048$. Similarly at point B (800 bar) the appropriate values are taken from tables 9a and 9c which give $dT_g/dP=0.015$ and $\Delta\beta/\Delta\alpha=0.037$. Accordingly, these data confirm that ineq (9) may be replaced by a stronger one which is obeyed here at both $P=P'=0$ and 800 bar:

$$\frac{dT_g}{dP} < \frac{\Delta\beta}{\Delta\alpha}. \quad (11)$$

Our average (over pressure) value, $dT_g/dP=0.021$, obtained from our variable formation history at $P=0$, is in close agreement with the value $(\partial T/\partial P)_\omega=0.020$ from dynamic compressibility measurements [34] and $(\partial T/\partial P)_\omega=0.022$ from dielectric measurements [6], on poly(vinyl acetate).

The fact that both sides of ineq (11) decrease markedly with increasing pressure suggests that dT_g/dP may vanish at a finite pressure. This possibility is also apparent in reference [32] on polystyrene data over a wider pressure range. According to the data, values of $\Delta\beta$ at T_g are nearly linear with T_g from which an extrapolation gives $\Delta\beta=0$ at a finite T_g corresponding to finite pressure. Also from dynamic compressibility

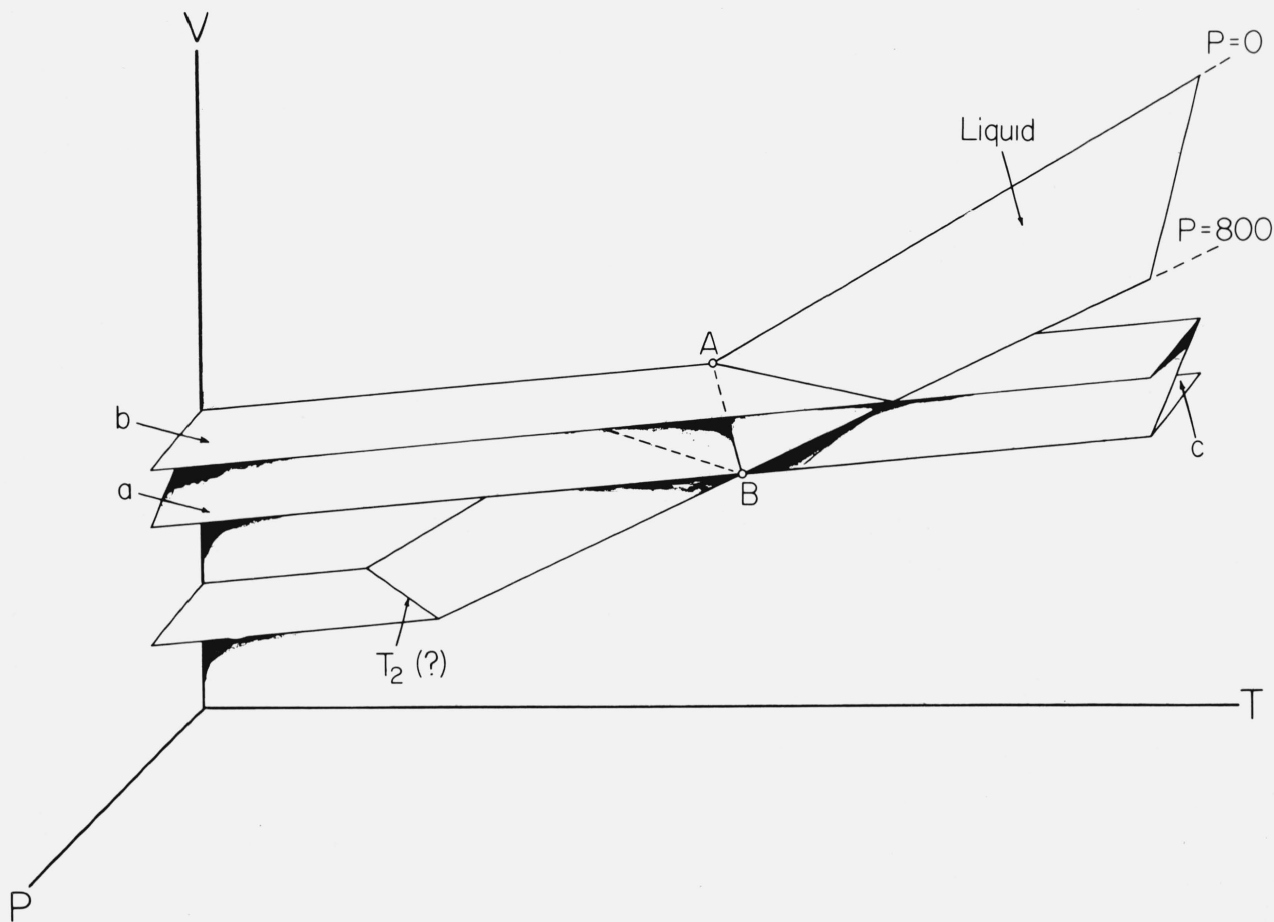


FIGURE 10. Schematic diagram illustrating liquid and glass surfaces *a* (variable formation), *b* (glass formed at atmospheric pressure), and *c* (glass formed at 800 bar) in PVT space.

data on poly(vinyl acetate) [34], linear extrapolations of $\Delta\beta$, the difference between high- and low-frequency limiting adiabatic compressibilities, which correspond to $\Delta\beta$, predict that this quantity vanishes at a finite pressure. Upon considering the data in this paper, from which we evaluate $\Delta\beta$ and $\Delta\alpha$ at T_g at the two points as given above, we find that $\Delta\beta$ at 800 bar is down 44 percent from its value at atmospheric pressure, whereas the corresponding value of $\Delta\alpha$ is down only 28 percent. This might suggest that $\Delta\beta$ could vanish while $\Delta\alpha$ remains finite. However a relation of thermodynamic stability among $\Delta\beta$, $\Delta\alpha$ and ΔC_p places restrictions on this possibility:

$$\Delta\beta \geq \frac{TV\Delta\alpha^2}{\Delta C_p}$$

so that unless ΔC_p approaches infinity while $\Delta\alpha$ remains finite, $\Delta\beta$ cannot approach zero. Since there is no reason to expect this behavior of ΔC_p , the behavior of $\Delta\beta/\Delta\alpha$ cannot be what is inferred from the 0–800 bar data, and experiments must be performed at higher pressures to find out what will happen.

The evaluation of ineq (11) as given earlier in this

section reveals a contradiction with respect to the free volume theory [2] as applied to time-temperature-pressure superposition, for which the characteristic temperatures are those approximating the isoviscous state. The free volume theory stipulates that the viscosity η is a single valued function of the free volume fraction which may be written explicitly in terms of the present temperature and pressure by

$$f = f_g + \alpha_f(T - T_{g0}) - \beta_f P \quad (12)$$

where T_{g0} is the value of T_g at atmospheric pressure. If the coefficients α_f and β_f are assumed to be given respectively by $\Delta\alpha$ and $\Delta\beta$, substitution in eq (12), followed by differentiation with respect to P at constant η (which is equivalent to constant f , since η is a single valued function of f) gives

$$\left(\frac{\partial T}{\partial P}\right)_\eta = \frac{\Delta\beta}{\Delta\alpha} \quad (13)$$

Since T_g may be taken to be the characteristic temperature for the isoviscous state, the above result is in apparent contradiction with in eq (11) for which the

right- and left-hand sides differ by nearly a factor of two as shown from these data. Accordingly, the eq (13) implies a single volume surface with respect to formation pressure, which is in contradiction with experimental evidence. This discrepancy has also been noted by Goldstein [9].

4.6. Experimental Uncertainties Including Estimates on T_g and T_g^*

In the absence of spurious effects the precision of the specific volume should depend upon the precision in measuring the experimental variables, which are temperature, pressure, and displacement of the mercury column. From the manufacturer's specifications the maximum deviations of the measurements of temperature and pressure are given as $\pm 0.25^\circ\text{C}$ and ± 2 bar. From replicate determinations on a fixed meniscus the maximum deviations on the height of the mercury column were found to be ± 0.002 cm. The relative precision (as determined by maximum relative deviation) may be approximated by

$$\left| \frac{\delta v}{v} \right| = \left| \frac{a_{10} \delta T}{a_{00}} \right| + \left| \frac{a_{01} \delta P}{a_{00}} \right| + \left| \frac{\pi r^2 \delta h}{W_s} \right| \quad (14)$$

where the capillary radius $r = 0.1$ cm, the sample weight $W_s = 6.27$ g and the values of the coefficients a_{ij} are taken from table 6. These uncertainties will have the greatest effect in the liquid region since the temperature and pressure coefficients are the largest. Applying eq (14) to the liquid region, the relative precision is $\delta v/v = \pm 0.028$ percent, for which the contributions from δT , δP , and δh are ± 0.017 percent, ± 0.010 percent, and ± 0.001 percent, of which the last is nearly insignificant. For the glasses the values of $\delta v/v$ decrease to (a) variable formation, ± 0.016 percent; (b) glass formed at atmospheric pressure, ± 0.014 percent; and (c) glass formed at 800 bar, ± 0.014 percent.

An alternative approach to evaluating the relative precision is to make use of the residual variation of the quadratic regression. (See Sec. 4.1.) The relative precision (as determined by relative standard deviation) of the specific volume may be approximated by $s/|a_{00}|$ where s is the estimated standard deviation of the residuals of the quadratic regression. It is noted that both of these methods are dependent upon the validity of the quadratic model. Also, it must be remembered that the maximum deviation and standard deviation usually differ by a factor between 2.0 and 2.5. The value of $s/|a_{00}|$ for the liquid is 0.013 percent, and the values for the glasses are (a) 0.009 percent, (b) 0.009 percent, and (c) 0.008 percent. The ratios of the precisions determined from maximum deviations to those by standard deviations vary from 2.2 for the liquid to 1.5 for glass b. The fact that these ratios are slightly smaller than expected indicates that the maximum deviations assumed for the experimental observables are too small, or that some unknown spurious effect was present. The latter could be a manifestation of irreversible expansion of the dilatometer

with pressure and temperature, which is possible, but not expected.

The relative precision (as measured by relative standard deviation) of the thermoexpansivities and compressibilities may be approximated by $\delta a_{10}/|a_{10}|$ and $\delta a_{01}/|a_{01}|$, respectively, where δa_{ij} is the estimated standard deviation of a_{ij} . For the liquid these relative standard deviations are 1.6 percent and 5.6 percent. For the glasses these values decrease to 0.42 percent and 0.44 percent averaged over the three histories. No explanation has been proposed to explain the large difference (4-fold for the thermoexpansivities and 12-fold for the compressibilities) between the corresponding values from liquid to glass.

The thermal expansion at atmospheric pressure was checked independently by hydrostatic weighing over the temperature range of 35–70 °C. At 40 °C the value obtained was down 3.6 percent from the corresponding dilatometer determination. However, the relative standard deviation in thermal expansion obtained by hydrostatic weighing was 7.8 percent compared with 1.6 percent given in the last paragraph. The principal reason for such a large value of the former was the difficulty in obtaining good temperature control at the higher temperatures. In view of the larger uncertainties with the hydrostatic weighing, the difference between the two determinations is hardly significant.

As pointed out in section 2.2, a correction was included in the formulation leading to eq (4) to account for the expansion of the dilatometer with temperature and pressure. This correction is small, and is often ignored by many investigators. Neglecting to include this correction gives a value for the thermal expansion at 40° and atmospheric pressure which is down 2.2 percent.

The accuracy of the specific volume measurements depends upon several sources of possible systematic error, or bias: the experimental observables given above, the reference specific volume determination (Sec. 2.3), mercury and glass expansion values (Sec. 2.2b), capillary bore and length measurements, weighings, and inhomogeneous dilatometer expansion.

Calibrations on temperature and pressure detecting apparatus showed that their systematic errors were small in comparison to their maximum deviations given above. Also measurements and calculations on the mercury and glass expansion values, capillary bore and length measurements, and weighings indicate that their contributions are negligible relative to those from the random deviations in temperature and pressure. Little is known about irregularities in the expansion characteristics of dilatometers; however, the expansion with temperature and pressure is generally believed to be homogeneous, and any possible contribution from inhomogeneous expansion is assumed to be minimal, or insignificant.

The contribution from the specific volume reference determination, apparently, is nonnegligible. An error in the reference value would bias all of the values obtained from the dilatometer measurements. The reference value was obtained by the usual hydrostatic

weighing procedure. As a result of water absorption by the sample, replicate measurements are difficult and time-consuming. Based on only three determinations at 40 °C (0.8488, 0.8485, and 0.8489 cm³/g) the average 0.8487 cm³/g was used as the reference value. Although statistics from only three values may not give results as reliable as desired, they do appear to have some utility, and appear to be reasonable, in this case. The average value has an estimated standard deviation and relative standard deviation of 0.00012 and .014 percent, respectively. A 95 percent confidence interval for the relative systematic error is $\pm 4.3 \times 0.014\% = \pm 0.060$ percent. Thus the overall relative accuracy is estimated to be $\pm (0.060\% + 2.0 \times 0.028\%) = \pm 0.116$ percent based on a relative precision of ± 0.028 percent for the liquid and an estimated bound of ± 0.060 percent on the systematic error. The factors 4.3 and 2.0 are the 97.5 percent points of the Students *t* distribution [40] with 101 and 2 degrees of freedom, respectively. The large factor 4.3 used in determining the systematic error bound results from only three available replicate determinations. In view of large sample to sample variations in polymers, in general, the bias factor 0.060 percent given above is not considered excessive. Similar calculations on the glass values will give slightly smaller values for their overall relative accuracy.

Since the relative uncertainties of the thermoexpansivities and compressibilities are large in comparison to those for the specific volume, they are not significantly influenced by errors in the reference determination. Accordingly, there should be no significant distinction between the imprecision and total uncertainty of these two quantities.

The uncertainty in T_g , (or T_g^*) which results from the uncertainties in the positions of the liquid and glass surfaces in *PVT* space, is one of the more useful, but one of the most difficult to evaluate. A statistical method giving the confidence limits on the intersection of the two quadratic surfaces used here would be extremely difficult to apply. In references [41, 42] methods are described which give the abscissa of the intersection of two linear regressions. These methods may be applied here to determine the confidence limits on T_g (or T_g^*) using paired linear regressions (liquid and glass) of the form $v = a + bT$ along each isobar. A FORTRAN Program for this calculation and examples are contained in reference [42].

The information required for these calculations consists of liquid-glass pairs of the following quantities: *N*, the number values; *a*, the intercept; *b*, the slope; \bar{T} , the average temperature; *s*, the standard deviation of the residuals of *v*; and

$$S^2 = \sum_{i=1}^N (T_i - \bar{T})^2.$$

Using the equal variance assumption, the confidence limits T^+ and T^- are the solutions of the quadratic equation

$$T^{\pm} = \frac{-B \pm \sqrt{B^2 - 4AC}}{2A}$$

where

$$A = (b_l - b_g)^2 - S_p^2 G^2 \left(\frac{1}{S_l^2} + \frac{1}{S_g^2} \right)$$

$$B = 2(a_l - a_g)(b_l - b_g) + 2S_p^2 G^2 \left(\frac{\bar{T}_l}{S_l^2} + \frac{\bar{T}_g}{S_g^2} \right)$$

$$C = (a_l - a_g)^2 - S_p^2 G^2 \left(\frac{1}{N_l} + \frac{1}{N_g} + \frac{\bar{T}_l^2}{S_l^2} + \frac{\bar{T}_g^2}{S_g^2} \right)$$

where *G* is the 97.5 percent point of the *t* distribution with N_p degrees of freedom (see [40], for example), where $N_p = N_l + N_g - 4$, and the pooled variance, S_p^2 , is defined as

$$S_p^2 = \frac{1}{N_p} [s_l^2 (N_l - 2) + s_g^2 (N_g - 2)] .$$

The subscripts *l* and *g* pertain to the liquid and glass as usual. (Note that \bar{T}_g here is not to be confused with the glass temperature.)

It is interesting to observe that the midpoint,

$$\frac{T^+ + T^-}{2} = -\frac{B}{A},$$

is nearly the same as, but not identical to, the estimate of T_g (or T_g^*) obtained from

$$T_g = -\frac{a_l - a_g}{b_l - b_g},$$

which is obtained by equating the two linear regressions. These two quantities are identical, however, in the limit $S_p \rightarrow 0$.

The results of this analysis are displayed in figure 11 where the 95 percent confidence bands are shown encompassing the estimated values of T_g or T_g^* as functions of pressure for the three histories. The values of T_g and T_g^* are taken from table 9 (shown also on fig. 7). The confidence bands, centered about T_g and T_g^* , are taken from the quadratic regressions of the calculated values of $\Delta T = T^+ - T^-$ with respect to pressure. The smoothed confidence bands shown on figure 11 range from 0.88 to 3.64 °C over the three histories. It was mentioned in section 4.2 that although the values of T_g and T_g^* are evaluated from the same sets of data for histories a and b at atmospheric pressure, and a and c at 800 bar, the intersections of the estimated values for which $T_g = T_g^*$ do not occur precisely at these pressures for the reason given. As seen from figure 11, however, the 95 percent confidence bands do overlap at 0 and 800 bar.

An additional reason for the inclusion of this figure is to illustrate how the proximity of the specific volume data to the estimated values of T_g or T_g^* influences their uncertainty. This effect is most clearly seen by curve

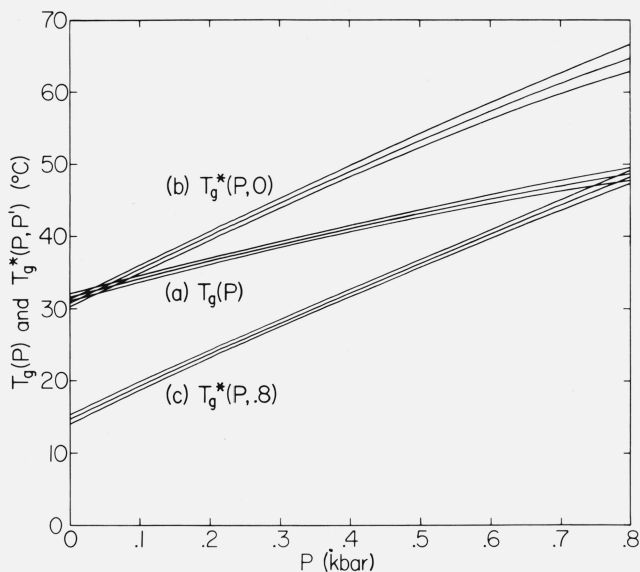


FIGURE 11. Transition map showing estimated values of T_g and T_g^* and 95 percent confidence limits versus pressure for histories (a) $P' = P$, (b) $P' = 0$, and (c) $P' = 0.8$ kbar.

b for which the specific volume data are displayed on figure 5. No problem arises from the proximity of the liquid data; however, with the glass there is a large region immediately below T_g^* for which there are no experimental data. At atmospheric pressure the difference between the estimated value of T_g^* and the closest experimental temperature in the glass is 10.68 °C. At 800 bar this difference increases to 54.61 °C. The confidence bands over this pressure range correspondingly go from 1.10 to 3.64 °C. This behavior illustrates the importance of obtaining data in the proximity of T_g (or T_g^*) in order to obtain an accurate estimate.

5. Concluding Remarks

The thermodynamic history by which a glass is formed has considerable influence on its structure and corresponding properties, as confirmed by the results of these experiments. The role of thermodynamic history was manifested by significant changes in the apparent glass temperature (T_g or T_g^*) the second order properties, and "permanent" densification.

In addition to the principal, or glass transition (sometimes referred to as α transition), observed in this work, secondary transitions, often called β transitions, have been reported from PVT measurements on certain polymers. The α transitions for amorphous polymers are taken to be manifestations of restrictions on the mobility of polymer chains, or long segments of the chains. The β transitions are attributed to restrictions on the mobility of short chain segments, or side group rotations. The PVT measurements of Quach and Simha [8] on polystyrene have revealed a β transition appearing within the glassy region with $dT_\beta/dP = 65.3$ °C/kbar. This value falls between the

values of dT_g/dP for their "low" and "high pressure" glasses. In our work there was some suspicion that the wide temperature range of observable relaxations using the constant formation history b ($P' = 0$) could be attributed to a β process. The observed relaxations were responsible for the absence of reported data at temperature immediately below T_g^* in figure 5. As pointed out in section 3.3, there was much less difficulty in obtaining pseudoequilibrium data immediately below T_g^* using history c ($P' = 800$ bar). From this information one might attribute the wide temperature range of observed relaxation with history b to a β process which would become "frozen in" at higher pressures. This could result from a large dT_β/dP as reported by Quach and Simha for which the α and β transitions would tend to merge at higher pressures.

On the other hand the evidence given by McCrum, Read, and Williams [43] precludes the possibility of a β transitions occurring within our experimental range. They give a $\log f$ (Hz) versus $1/T$ plot for the β relaxation taken from various dynamic data. Using the dashed curve of their figure 9.4 estimated to be of the form $\log f = 13.3 - 2.1 \times 10^{-3}/T$, and using a conservative estimate of $\log f = -3$ gives a value of $T_\beta = -145$ °C, which is well below our experimental range (-30 to 100 °C). With a similar plot for polystyrene [44] estimated to be of the form, $\log f = 25.2 - 8.0 \times 10^{-3}/T$, and using the same value of $\log f$ gives $T_\beta = 11$ °C. The value obtained from extrapolating the PVT data of Quach and Simha to atmospheric pressure gives $T_\beta = 3$ °C. Aside from other possible discrepancies, the difference between these values indicates that our choice of the value of $\log f$ was too conservative. Accordingly, this evidence would appear to preclude the possibility of a β transition being observed over our experimental range. As stated in section 3.3, the difficulty in obtaining pseudoequilibrium data close to T_g^* for history b apparently arises from the manner in which the data were observed.

With respect to the First Ehrenfest Relation (eq (8), Sec. 4.5), it should be remembered that this relation may be considered to be a tautology when applied to liquid-glass systems using the apparent values of the second order properties, obtained from the data, which are not necessarily the proper thermodynamic ones. If the proper thermodynamic properties are used the First Ehrenfest Relation fails for the isoviscous state, and must be replaced by its corresponding inequality

$$\frac{dT_g}{dP} < \frac{\Delta\beta}{\Delta\alpha} \quad (11)$$

Obedience of ineq (11) is tantamount to higher densities with increasing formation pressures, as illustrated by these experiments. This result has been shown to be in contradiction with the free volume theory. The fact that the volume of a glass decreases with the formation pressure, and the entropy, apparently, does not (which is tantamount to the satisfaction of ineq (11) and eq (7)), supports an entropy rather than a volume basis for the transition or relaxation processes.

The results of these and related experiments have

technological importance. With highly densified glasses one would expect corresponding increases in cohesive energy density giving harder and stronger glasses along with larger refractive indices.

Note added in proof: From graphical C_p data [46] on poly(vinyl acetate) taken through T_g a value of $\Delta C_p = 0.097$ cal/g-K (0.405J/g-K) is obtained at $T = T_g$. Applying this value to eq (7) gives for the right-hand side 0.027 °C/bar, which is in agreement with our value of dT_g/dP at atmospheric pressure. (See table 9a.) This result confirms the validity of eq (7), which implies the existence of a single entropy surface with respect to formation pressure for this polymer.

The authors acknowledge and appreciate the assistance from H. V. Belcher and M. R. Brockman in obtaining these data, from J. J. Filliben in statistical analysis, and from R. S. Marvin in planning this work and for suggestions in preparing this manuscript.

6. References

- [1] Gee, G., *Contemp. Phys.* **11**, 313 (1970).
- [2] Ferry, J. D., *Viscoelastic Properties of Polymers*, Chapt. 11 (John Wiley and Sons, New York, 1970).
- [3] Kovacs, A. J., *J. Polymer Sci.* **30**, 131 (1958).
- [4] Bianchi, U., Turturro, A., and Basile, G., *J. Phys. Chem.* **71**, 3666 (1967).
- [5] Matsuoka, S., and Maxwell, B., *J. Polymer Sci.* **32**, 131 (1958).
- [6] O'Reilly, J. M., *J. Polymer Sci.* **57**, 429 (1962).
- [7] Hellwege, K. H., Knappe, W., and Lehmann, P., *Kolloid Z. und Z. für Polymere* **183**, 110 (1963).
- [8] Quach A., and Simha, R., *J. Appl. Phys.* **42**, 4592 (1971).
- [9] Goldstein, M., *J. Phys. Chem.* **77**, 667 (1973).
- [10] Martin, G. M., and Mandelkern, L., *J. Appl. Phys.* **34**, 2312 (1963).
- [11] McKinney, J. E., and Penn, R. W., *Rev. Sci. Instr.* **43**, 1211 (1972).
- [12] Forsythe, W. E., *Smithsonian Physical Tables*, p. 152, Smithsonian Institution, Washington, D.C. (1954).
- [13] Bridgman, P. W., *Am. J. Sci.* **10**, 359 (1925).
- [14] Carnazzi, P., *Nuovo Cimento* **5**, 180 (1903).
- [15] See for example, Tanford, C., *Physical Chemistry of Macromolecules* (Wiley and Sons, New York, 1961), p. 407.
- [16] Kurata, M., Iwana, M., and Kamada, K., in *Polymer Handbook*, Ed. Broadrup, J., and Immergut, E. H. (Interscience, New York, 1966, Section 4), p. 16.
- [17] Burrel, H. and Immergut, E. H., in reference 46, Section 4, p. 347.
- [18] Fox, T. G., Gratch, S., and Loshaek, S., in *Rheology*, F. R. Eirich, Ed., Vol. **I**, Chapt. 12 (Academic Press, New York, 1956).
- [19] Fox, T. G., and Loshaek, S., *J. Poly. Sci.* **15**, 371 (1955).
- [20] Magill, J. M., *J. Appl. Phys.* **35**, 3249 (1964).
- [21] Ref. [2], p. 519.
- [22] Bauer, N., in *Physical Methods of Organic Chemistry*, A. Weissberger, Ed., Vol. **I**, Chapt. 6 (Interscience, New York, 1949).
- [23] *Standard Density and Volumetric Tables*, Circular of the Bureau of Standards, No. 19 (1924).
- [24] Goldbach, G., and Rehage, G., *J. Polymer Sci., Part C*, **16**, 2289 (1967).
- [25] Tait, P. G., *Physics and Chemistry of the Voyage of the H. M. S. Challenger* (University Press, Cambridge, 1900), Vol. **II**, Part IV, *Scientific Papers LXI*, Vol. **II**, p. 1 (1888).
- [26] Wood, L. A., *Polymer Letters* **2**, 703 (1964).
- [27] Gee, G., *Polymer* **7**, 177 (1966).
- [28] Hilsenrath, J., Ziegler, G. G., Messina, C. G., Walsh, P. J., and Herbold, R. J., OMNITAB, a computer program for statistical and numerical analysis, Nat. Bur. Stand. (U.S.), Handb. 101, 93 pages (April 1968).
- [29] Draper, N. R., and Smith, H., *Applied Regression Analysis* (John Wiley and Sons, New York, 1966), p. 71.
- [30] Davies, R. O., and Jones, G. O., *Adv. Phys.* **2**, 370 (1953).
- [31] Simha, R., and Boyer, R. F., *J. Chem. Phys.* **37**, 1003 (1962); Boyer, R. F., and Simha, R., *Polymer Letters Edition* **11**, 33 (1973).
- [32] Boyer, R. F., in *Styrene polymers*, R. F. Boyer, Ed., *Ency. Polymer Sci. and Tech.* Vol. **13**, 1970, p. 297.
- [33] Turnbull, D., *Contemp. Phys.* **10**, 473 (1969).
- [34] McKinney, J. E. and Belcher, H. V., *J. Res. Nat. Bur. Stand. (U.S.)*, **67A** (Phys. and Chem.), No. 1, 43-53 (Jan.-Feb. 1963).
- [35] Kimmel, R. M., and Uhlman, D. R., *J. Appl. Phys.* **41**, 2917 (1970).
- [36] Reference [2], p. 314.
- [37] Reference [2], p. 316.
- [38] Gibbs, J. H., and DiMarzio, E. A., *J. Chem. Phys.* **28**, 373 (1958).
- [39] Passaglia, E., and Martin, G. M., *J. Res. Nat. Bur. Stand. (U.S.)*, **68A** (Phys. and Chem.), No. 3, 273-276 (May-June 1964).
- [40] Beyer, W. H., Ed., *Handbook of Probability and Statistics*, p. 82, Chemical Rubber Co., Cleveland, 1966.
- [41] Kastenbaum, M. A., *Biometrics* **15**, 323 (1959).
- [42] Filliben, J. J. and McKinney, J. E., *J. Res. Nat. Bur. Stand. (U.S.)*, **76B** (Math. Sci.), Nos. 3 & 4, 179-192 (July-Dec. 1972).
- [43] McCrum, N. G., Read, B. E., Williams, G., *Anelastic and Dielectric Effects in Polymeric Solids*, (Wiley and Sons, New York, 1967), p. 304.
- [44] *Ibid*, p. 414.
- [45] Marvin, R. S., and McKinney, J. E., in *Physical Acoustics*, W. P. Mason, Ed., (Academic Press, New York, N.Y., 1965, Vol. **2B**, Chapt. 9).
- [46] Vol'kenshtein, M. V., in *Structure of Glass*, Vol. 2, Consultants Bureau, New York, 1961, p. 111 (Translation).